

FINAL TECHNICAL REPORT

Submitted to
UNITED STATES DEPARTMENT OF ENERGY
Morgantown Campus
3610 Collins Ferry Road
PO Box 880
Morgantown, WV 26507-0880
Program Manager: Otis Mills

DOE Award No. DE-FE0027102

PLASMA ARC GASIFICATION BASED RARE EARTH ELEMENT RECOVERY FROM COAL FLY ASH

Principal Investigator: Jay E. Renew, Ph.D., P.E.
jrenew@southernresearch.org
(205) 908-3527

Submitting Official: Ken Jeffers, P.E.
Manager – Resource Recovery
kjeffers@southernresearch.org
(205) 581-2166

Report Submitted:
8 September 2017

Report No. DOE-SR-FE-27102

DUNS # 006900526

Recipient Organization:
SOUTHERN RESEARCH INSTITUTE
2000 NINTH AVENUE SOUTH
BIRMINGHAM, AL 35205-2708

DISCLAIMER

This report was prepared as an account of work sponsored by an agency of the United States Government. Neither the United States Government nor any agency thereof, nor any of their employees, makes any warranty, express or implied, or assumes any legal liability or responsibility for the accuracy, completeness, or usefulness of any information, apparatus, product, or process disclosed, or represents that its use would not infringe privately owned rights. Reference herein to any specific commercial product, process, or service by trade name, trademark, manufacturer, or otherwise does not necessarily constitute or imply its endorsement, recommendation, or favoring by the United States Government or any agency thereof. The views and opinions of authors expressed herein do not necessarily state or reflect those of the United States Government or any agency thereof.

EXECUTIVE SUMMARY

Southern Research, as the primary awardee, with sub-awardees ArcSec Technologies, LLC (ArcSec) and Reaction Engineering International (REI) have investigated a plasma arc based thermal process intended to concentrate rare earth elements (REE) from coal fly ash. This work was conducted as part of DOE-NETL's program to advance domestic coal and associated by-products – specifically post-combustion coal ash for this project – as viable sources for the recovery of rare earth materials. Successful demonstration of the technology would contribute to the effort for realizing a competitive, domestic REE value chain thereby reducing U.S. dependence on foreign supply, maintaining national security interests, and creating opportunities for economic growth.

The originally proposed concept included two technology options – 1) a smelting process and 2) a smelting plus vaporization and condensation process. For both options, coal fly ash would be smelted in a plasma arc heated furnace under reducing conditions to separate ash into molten slag and reduced metal (primarily iron) phases. During smelting, it was expected that the REE would also be reduced to metals and partition mostly to the iron phase. In a continuous process, the slag would be removed and the molten metal poured into a mold or casting table and cooled. Initial indications show that the slag material can be converted into additional, environmentally benign products for sale, or can be sequestered long-term as a highly stable waste residual. The purpose of the vaporization/condensation option was to separate individual REE and produce additional REE-enriched metal fractions. For this process, the molten metal was to be further heated after smelting to vaporization temperatures. As in a distillation process, the vapors would rise up through the furnace and be condensed in a staged manner using a specialized collection system coupled to the furnace exit.

During the first year of work, sample coal ash feedstocks were acquired and characterized, feasibility of the smelting process was evaluated in bench-scale experiments, and the vaporization/condensation process was investigated through equilibrium and CFD modeling studies. From the feedstock characterization, REE content for the coal ash samples obtained was measured to be in the range of 302 – 1219 ppm with average at 537 ppm. Though it was successfully demonstrated that ash could be separated into slag and metal phases, the bench-scale experiments were only marginally successful at collecting REE in the metal phase. Producing REE concentrates near the DOE goal of 2%, however, has not been achieved. From the modeling studies, the vaporization/condensation process was predicted to be effective for separating individual REE and producing enriched metal fractions with total REE content higher than 2%, provided the smelting process performed as intended.

Supplemental smelting experiments and thermodynamic modeling studies, conducted during the second year of work, indicated a number of technical modifications that could lead to producing higher REE concentrates from coal ash. The strategy shifted to reducing as much of the ash oxides to metals as possible, leaving the REE more concentrated in the remaining slag. Results from later experiments based on the modified approach showed improvements in REE recovery and concentration levels in smelted products. SEM-EDS analyses on product specimens showed agglomerations of reduced metal REE crystals at much larger length-scales as compared to REE content in raw ash. Because the project team did not have equipment suitable for further proving-out the modified concept, and since the originally proposed smelting process had not proven to be viable, a test unit for further process development was designed which will provide broad operating flexibility for conducting well-controlled experiments under a wide range of thermal and atmospheric conditions. The proposed test unit design is intended to be a significant improvement for rigorously demonstrating that the modified technology is viable for extracting and concentrating REE from coal fly ash.

TABLE OF CONTENTS

EXECUTIVE SUMMARY	3
1. INTRODUCTION AND PROJECT OBJECTIVES	5
2. PROPOSED TECHNOLOGY SUMMARY	6
2.1 Ash Smelting Process	6
2.2 Smelting Plus Vaporization/Condensation Process	7
2.3 Environmental Impact	8
3. FEEDSTOCK SAMPLING AND CHARACTERIZATION SUMMARY	10
4. FEASIBILITY STUDY REVIEW	13
4.1 Bench-scale Experiments Summary	13
4.2 Computational Modeling Summary	17
4.3 Economic Analysis	20
5. TECHNOLOGY REASSESSMENT	22
5.1 Review of Fundamentals	22
5.2 Review of Related Applications	23
5.3 Supplemental Modeling	24
5.4 Adjustments to Proposed Technology	29
5.5 Supplemental Experiments	31
6. TEST UNIT DESIGN	39
6.1 Design Approach and Key Inputs	39
6.2 Design Concept and Specifications	40
6.3 Preliminary Cost Estimates	41
7. CONCLUSIONS	42
8. RECOMMENDED FUTURE WORK	44
9. REFERENCES	45

1. INTRODUCTION AND PROJECT OBJECTIVES

This report is submitted to satisfy the Phase 1 Task 5 Milestone as described in the Statement of Project Objectives for US DOE Award DE-FE0027102. Presented herein is a final summary of findings and results from a comprehensive effort to demonstrate feasibility of proposed technology for recovering and concentrating rare earth elements (REE) from coal fly ash and to prepare a design package for a pilot demonstration unit. This project has been funded under DE-FOA-0001202, Area of Interest (AOI) 2: Pilot-Scale Technology to Economically Separate, Extract, and Concentrate Mixed REE from Coal and Coal Byproduct Solids. The project team consists of Southern Research as the primary awardee with sub-awardees ArcSec Technologies, LLC (ArcSec) and Reaction Engineering International (REI). Project supporters included the University of Utah, which conducted bench-scale plasma smelting experiments and provided technical advisement, Headwaters Resources, which provided sample materials and analysis, and Southern Company Services, which provided technical advisement.

The overall project objective was to develop and demonstrate an innovative process for extracting and recovering REE from coal or coal-associated solid material feedstocks (having minimum REE content of 300 ppm) into a final product having a total mixed REE concentration approaching 2% by weight. For this work, post-combustion coal fly ash was the selected feedstock of choice, and the proposed recovery technology relied on a plasma arc smelting process to separate ash into molten slag and reduced metal (primarily iron) phases where reduced REE are expected to partition to the reduced metal phase.

To achieve this end, the prescribed work tasks (listed and summarized in Table 1) included acquiring and characterizing various feedstocks (Task 2), performing a comprehensive feasibility study (Task 3), and preparing a design package for a demonstration unit (Task 4). Numerous coal ash samples were to be sought, representing a broad spectrum of available feedstocks, with the goal of obtaining the highest possible REE content to provide the best chance of achieving the DOE concentration goal. As an AOI 2 project, both technical and economic feasibility of the proposed technology were to be evaluated and demonstrated for proceeding with a pilot-scale application. The study would also include identifying the scope of effort necessary for advancing to a commercial application. Upon successful demonstration of feasibility, a detailed design package for a pilot-scale demonstration unit was to be prepared. The pilot system was to be designed with built-in operating flexibility to accommodate ash feedstock composition variability and to minimize or reduce any detrimental environmental, safety, and health impacts. Results and findings from Tasks 2–4 are further described and summarized in Sections 3–6.

Table 1. Summary of project tasks.

Task No.	Description
Task 1.0	Project Management Planning
Task 2.0	Sampling and Characterization for Proposed Feedstocks
Task 2.1	Sampling and Characterization plan
Task 2.2	Sampling and Characterization plan implementation
Task 3.0	Feasibility Study
Task 3.1	Bench-scale smelting tests
Task 3.2	Computational modeling of the vaporization and condensation process
Go/No-Go Decision Point	
Task 4.0	Design of Pilot-Scale Unit
Task 5.0	Final Summary Report

2. PROPOSED TECHNOLOGY SUMMARY

REE have been found in US domestic coal fly ashes in low concentrations (average ~500 ppm), being encapsulated and evenly distributed in amorphous, glassy alumina-silicate phases (Franus, Wiatros-Motyka, & Wdowin, 2015; Hower et al., 2013; Querol, Fernandez-Turiel, & Lopez-Soler, 1995). To recover REE from coal-based feedstocks, conventional separation processes such as sieve screening, gravity separations, magnetic separations, and froth flotation have been prescribed in various arrangements and combinations to remove as much of the undesired materials as possible before extracting the rare earth minerals. Once isolated, the high-value fraction is usually subjected to hydrometallurgical processing – typically acid leaching – to dissolve and extract the REE into solution, which could then be precipitated, filtered, and dried as a mixed rare earth oxide (pre-)concentrate. However, leaching REE from coal ash by traditional methods is difficult due to the chemical stability of the alumina-silicate matrix, and this entire glassy phase would have to be leached to completely extract the REE minerals (Hower et al., 2013).

For this work, the approach was to exploit differences in melting and boiling point temperatures for the various constituents to thermally separate and concentrate REE from coal ash gangue materials. The proposed REE recovery technology was, therefore, a pyrometallurgical process with two options:

1. Smelting in a reducing environment to separate coal ash into slag and a reduced metal (primarily iron) product where reduced rare earth metals collect and concentrate in the metal phase.
2. The smelting process plus vaporization of the rare earth enriched metal product followed by sequential condensation of the vapors to achieve separation of individual REE and produce additional metal fractions with further REE enrichments.

Both options rely on plasma arc technology to achieve the high temperatures required to smelt coal ash (1500 – 2000 °C) and vaporize the REE-containing metal product (2000 – 3500 °C). The general system arrangement would be a closed plasma furnace equipped with graphite electrodes to generate the plasma arc. Molten material – slag and metal – would be drawn off through ports fitted in the lower portion of the furnace. Vapors produced during processing would exit the upper furnace section, which would be ducted to an exhaust gas scrubbing system to prevent harmful emissions prior to venting. The energy input requirements for a commercial unit have been estimated at 800 kW per ton of ash feedstock. The two process options are discussed with further detail in the following sections.

2.1 Ash Smelting Process

The basic flow diagram for the smelting process is presented in Figure 1.

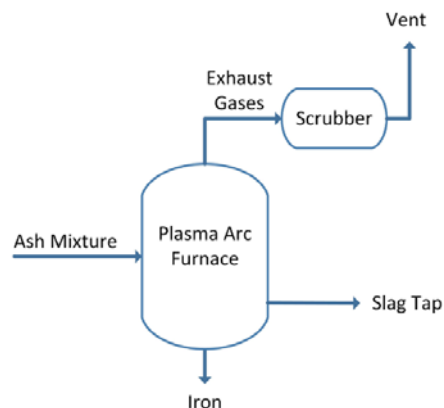
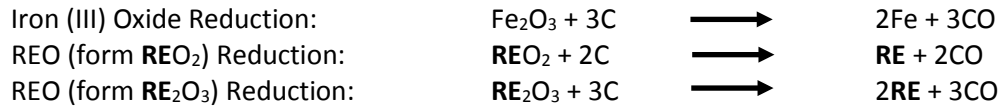


Figure 1. Process flow for smelting-only process option.

A mixture of ash, flux, and carbon is first charged to the plasma furnace. The purpose of flux addition – lime, limestone and/or silica – is to reduce both the ash melting temperature and the viscosity of the melt, which improves flow characteristics. The flux addition ratio is adjusted to the raw ash chemistry, specifically silica and alumina content. Carbon – likely in the form of metallurgical coke – is the reducing agent to convert iron oxide (Fe_2O_3), in the ash, to iron metal (Fe) and REE (assuming they occur in ash as rare earth oxides – REO) to rare earth metals. The key reduction chemical reactions assumed to occur during smelting are as follows:



where “RE” represents a given rare earth element/atom. The reduced iron is intended to serve as a collector metal for the reduced rare earth metals. Considering the range of iron and REE content of the fly ash feedstocks evaluated, best-case REE concentrations in the smelted metal product would be in the range of 1–2% (see Section 3).

Once charged, the furnace is sealed to the atmosphere, and the plasma-arc system is activated to heat the ash mixture to a molten state (at 1500 – 2000 °C). While molten, slag and reduced iron separate into distinct layers with the slag on top and iron on bottom. When the separation is complete, the molten slag is tapped off or poured out from the furnace, cooled, and solidified. The molten iron can then be collected from the furnace bottom (e.g. poured into a mold, cooled, and solidified). Gases produced during the smelting process – primarily carbon monoxide (CO) with small quantities of sulfur dioxide (SO_2) and possible break-through metal vapors – are treated in an exhaust gas scrubbing system downstream from the furnace exit prior to final venting.

2.2 Smelting Plus Vaporization/Condensation Process

The basic flow diagram for the smelting plus vaporization/condensation process is presented in Figure 2.

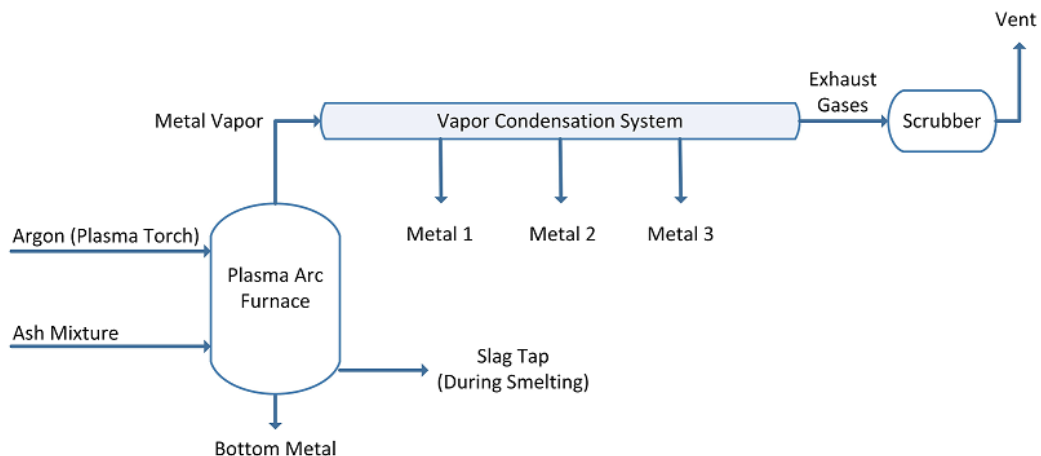


Figure 2. Process flow for the smelting plus vaporization and condensation process option.

The purpose of the smelting plus vaporization and condensation process is to refine the metal product from smelting by separating individual REE and producing additional metal fractions, further enriched in REE. The vaporization step would be carried-out in the same plasma furnace used during the ash-smelting

step. After first smelting raw ash, the molten slag layer is removed, and the remaining metal pool at the bottom of the furnace is further heated to vaporization temperatures. As in a distillation process, the vapors rise up through the furnace and are then condensed in a staged manner using a specialized collection system, which would be located between the furnace exit and the scrubbing system. For this operation, the gas volumes generated from vaporizing metals are low, and an added plasma torch would provide a flow of heated gas (argon) to sufficiently maintain high temperatures in the upper furnace section to prevent condensation of metal vapors before reaching the furnace exit and collection system. From the collection system, any uncondensed vapors are treated in the exhaust gas scrubber system before final venting.

2.3 Environmental Impact

The primary goal of a recycling process is to minimize the fiscal and environmental costs of a product compared to a raw production method. In this case, the added value of national security plays an important role, since the vast majority of REE production is performed overseas (typically in countries with significant political risk). Given the severe impacts of mining on the environment, the process of reclaiming REE from coal ash is inherently advantageous in terms of environmental costs. The mining has already been completed and attributed to the primary cost of coal production. The remaining environmental costs are localized to the smelting and cleanup processes required for REE production from the ash by-product of coal combustion.

The environmental effects of the smelting/vaporization process will be similar to a commercial electric arc smelter operation. In both cases a substantial amount of energy is required to convert solid, primarily inorganic feedstock, into a molten phase. The energy required for this operation may be produced from renewable sources to mitigate obvious effects of increased power requirements. However, in the likely event that near-term processes rely on fossil energy sources, it can be assumed that increases in natural gas energy are required (as well as associated emissions and environmental effects from natural gas production). Otherwise, a second option is diminished net electrical output from the associated coal power plant that can be expected in return for production of coal ash derived REE products.

Direct environmental costs will be attributed primarily to the off-gas emissions and downstream cleanup equipment. During the smelting process, gas emissions will primarily consist of CO as the various ash oxides are reduced to metals by added carbon. The off-gases will initially be passed through a cleaning system and then burned for process heat/energy. Conventional cleaning equipment will be used to remove contaminants and any harmful volatilized compounds from the ash feed, such as trace metals or residual sulfur compounds. The associated cleaning media (water and solid adsorbents) will be recycled as much as possible and treated prior to disposal as is done with conventional water treatment and land fill disposal for packed bed media.

The slag from the smelting process can be beneficially used as aggregate for construction materials, or it can be transformed into rock wool. If the slag portion must instead be disposed of, a key environmental benefit is that this by-product (including any additional waste from the flux and reductant additives) is far less susceptible to leaching of harmful contaminants as compared to disposed raw ash. It is expected that the slag would pass all TCLP tests (in tests conducted by the Georgia Institute of Technology, similar slag fractions produced from municipal solid waste combustion ash passed all TCLP criteria (Report, 1997)). The thermal plasma process vitrifies the slag portion, producing a highly stable by-product, and its resulting volume is far less than that of the raw ash – vitrified slag density is $\sim 100 \text{ lb/ft}^3$ while the density of ash-coke-lime mixture is $\sim 40 \text{ lb/ft}^3$. For a commercial-sized REE recovery unit, calculations

demonstrated that the daily volume of vitrified slag produced was ~44% less than the initial volume of raw ash feed. The combination of lower material volume and more opportunities for beneficial use results in significantly decreased waste storage requirements for slag as compared to coal ash. Another environmental benefit is that, unlike most REE recovery strategies, the proposed thermal process is not a water-intensive treatment process.

3. FEEDSTOCK SAMPLING AND CHARACTERIZATION SUMMARY

In previous work, the REE content of US coal ashes has been shown to be highly variable with concentrations ranging from 100 – 1600 ppm (Blissett, Smalley, & Rowson, 2014; Ketris & Yudovich, 2009; Mardon & Hower, 2004; Mayfield & Lewis, 2013; Seredin & Dai, 2012). Eastern US bituminous coal ashes (particularly from Central Appalachian coals) have been characterized with REE content to be on the higher end with average concentration at ~500 ppm (Blissett et al., 2014; Ketris & Yudovich, 2009; Mardon & Hower, 2004; Mayfield & Lewis, 2013; Seredin & Dai, 2012). Sources for ashes with high-end REE concentrations (e.g. > 1000 ppm) are limited, but a well-known example is the Fire Clay coal seam of Eastern Kentucky. Eastern bituminous coal ashes also contain sufficient levels of iron oxide (Fe_2O_3), which is important because, as previously noted, reduced iron would serve as the primary REE collector metal for the smelting process. However, the range of iron content in the feedstock ash must be appropriately balanced to maximize the REE concentration in the smelted metal product – if iron content is too low, REE collection will be disadvantaged; if too high, the REE concentration may be diluted below the 2% goal. Figure 3 is a graph of the theoretical maximum weight % of REE in the metal product vs. total REE content in the raw ash (assuming 100% REE recovery) with plots for various ash Fe_2O_3 content.

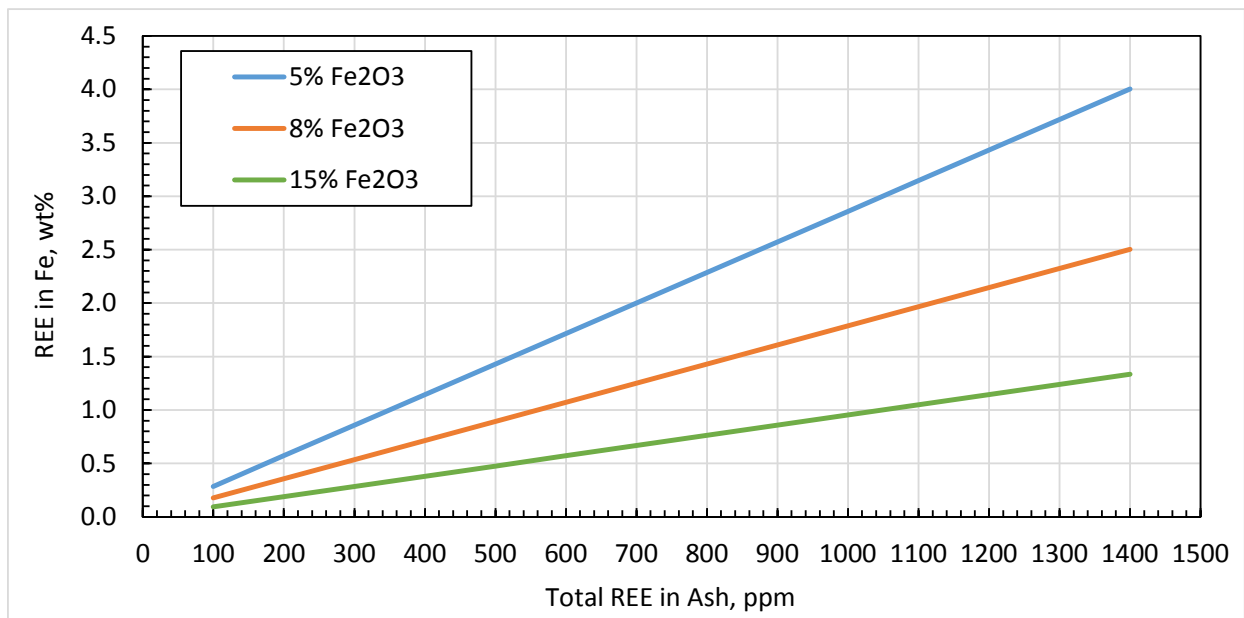


Figure 3. Maximum theoretical weight % of REE in the metal product (reduced Fe) vs total REE in ash.

To produce REE concentrates approaching the DOE goal, REE content in the ash would necessarily be greater than 600 ppm and 1000 ppm for ash Fe_2O_3 levels of 5% and 8%, respectively. Therefore, feedstocks acquired for the experimental work were targeted to meet the following criteria:

- Ash from combustion of Appalachian bituminous coals.
- REE content as high as possible; greater than 600 ppm.
- Fe_2O_3 content in the range of 5 – 10%.

Ultimately, coal ash feedstock samples from 11 sources were collected and characterized. Summary source information on the samples acquired with total REE content measured is included in Table 2.

Table 2. Summary of coal ash feedstock sources.

No.	Type	Ash Source	Coal Source	Total REE, mg/kg
1	Fly Ash	First Energy, WH Sammis Power Plant, OH	Cent/North App (WV, PA)/PRB blend	391
2	Fly Ash	Brayton Point Power Station, MA	Columbia SA/Central App blend	432
3	Fly Ash	Orlando Utilities Com, Stanton Energy Center, FL	IL Basin	329
4	Fly Ash	AEP, Mountaineer Power Plant, WV	Central App (WV)	424
5	Fly Ash	AEP, Mitchell Power Plant, WV	Central App (WV)	483
6	Fly Ash	Southeastern US Power Plant	IL Basin	388
7	Fly Ash	EKPC, JS Cooper Power Station, KY	Central App (KY, Fire Clay)	717
8	Fly Ash	SCANA, Williams Station, SC	Central App (KY, Fire Clay)	682
9	Stoker Ash	Kentucky State University	Central App (KY, Fire Clay)	1219
10	Weathered Ash	Brayton Point Power Station, MA	Columbia SA/Central App blend	302
11	Bottom Ash	Brayton Point Power Station, MA	Columbia SA/Central App blend	156

Table 3 presents summary results from the sample characterization including ranges for total REE, selected individual REE, bulk chemistry (oxides), and crystalline phases of interest. Note that the bottom ash sample was not included for determining average and range values.

Table 3. Summary results from the characterization of coal fly ash feedstock samples.

Component	Determined by	Units	Average	Low	High
Total REE	ICP-MS	mg/kg	537	302	1219
Scandium (Sc)	ICP-MS	mg/kg	33.4	26.1	45.7
Yttrium (Y)	ICP-MS	mg/kg	80.3	45.4	193.1
Lanthanum (La)	ICP-MS	mg/kg	81.1	43.4	185.2
Cerium (Ce)	ICP-MS	mg/kg	170.6	88.7	395.4
Praseodymium (Pr)	ICP-MS	mg/kg	20.1	10.6	47.4
Neodymium (Nd)	ICP-MS	mg/kg	75.5	40.4	177.2
Europium (Eu)	ICP-MS	mg/kg	3.4	2.1	5.3
Terbium (Tb)	ICP-MS	mg/kg	2.6	<0.8	5.2
Dysprosium (Dy)	ICP-MS	mg/kg	15.0	8.4	36.0
Erbium (Er)	ICP-MS	mg/kg	8.9	4.9	21.7
SiO ₂	XRF (oxides)	wt%	52.5	42.7	60.1
Al ₂ O ₃	XRF (oxides)	wt%	25.0	21.1	32.5
Fe ₂ O ₃	XRF (oxides)	wt%	12.5	4.8	24.5
CaO	XRF (oxides)	wt%	2.8	1.2	5.2
Amorphous	XRD	wt%	72.7	64.0	80.6
Quartz	XRD	wt%	12.3	6.8	17.2
Mullite	XRD	wt%	5.6	2.5	9.7
Hematite	XRD	wt%	4.3	2.5	5.4

From Table 3, the fly ash oxide chemistry was determined by X-ray Fluorescence (XRF), and the characterization results demonstrated that ash is a mixture of mineral oxides with silica (SiO_2), alumina (Al_2O_3), iron oxide (Fe_2O_3), and calcium oxide (CaO) comprising 90–95% of its total composition. Figure 4 presents graphically, with additional detail, the average oxide composition of bituminous coal fly ash (based on the samples acquired) with constituent amounts given as weight percentages.

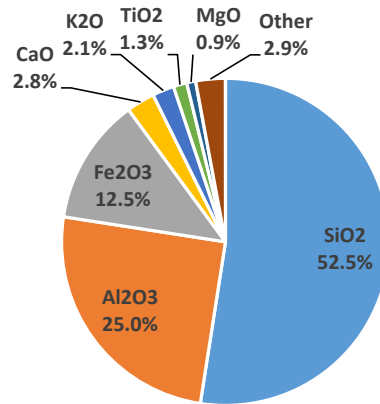


Figure 4. Average oxide composition of bituminous coal fly ash with constituents given as weight percentages.

Also from Table 3, the average total REE concentration, as determined by Inductively Coupled Plasma-Mass Spectrometry (ICP-MS), for the coal ashes collected was 537 mg/kg (ppm). Generally, coal fly ash was found to be richer in the “light” rare earth elements (LREE – La, Ce, Pr, Nd, Sm) as compared to the “heavy” rare earth elements (HREE – Eu, Gd, Tb, Dy, Ho, Er, Tm, Yb, Lu, and Y) – LREE content was about 2.5 times that of HREE content. Scandium (Sc) was neither classified as LREE or HREE, and average content was found to be 7% of the total REE. Figure 5 presents the division in coal ash by weight percentages among LREE, HREE, and Sc.

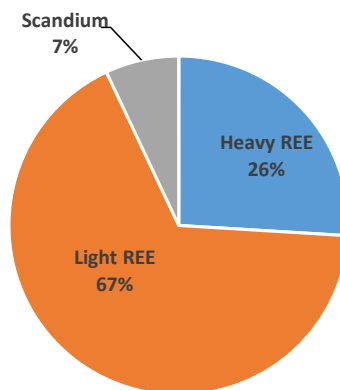


Figure 5. Average division among LREE, HREE, and Scandium in coal ashes collected for the present work.

Regarding the crystalline phases, as determined by X-ray Diffraction (XRD), fly ash is primarily amorphous with quartz (SiO_2), mullite ($3\text{Al}_2\text{O}_3 \cdot 2\text{SiO}_2$ or $2\text{Al}_2\text{O}_3 \cdot \text{SiO}_2$), and hematite (Fe_2O_3) being the next most common phases present. Higher fractions of mullite tend to increase the ash melting point. As noted in Section 2.1 lime (CaO) can be added to the ash to lower the melting point.

4. FEASIBILITY STUDY REVIEW

Feasibility of the two process options was investigated separately with the smelting-only process being evaluated through bench-scale experiments and the vaporization/condensation process evaluated through computational modeling.

4.1 Bench-scale Experiments Summary

The general experimental approach to demonstrating feasibility of the smelting process initially included the following activities:

- Selecting fly ash feedstocks having characteristics that provided a high probability of achieving the study objectives.
- Determining the test conditions necessary for successfully smelting fly ash sample preparations.
- Demonstrating the ability to produce separate slag and reduced metal phases.
- Demonstrating the ability to liberate, reduce, and collect REE in the reduced metal phase.

The fly ash feedstocks selected for bench-scale experiments are listed in Table 4, including key characteristics and theoretically best possible final smelted product REE concentration. The selected feedstocks were chosen primarily for their relative appreciable REE content and iron oxide content being on the low end of the range for all acquired samples.

Table 4. Feedstocks selected for bench-scale smelting experiments.

No.	Feedstock Source	Total REE, mg/kg	Fe ₂ O ₃ , %	Theoretical. Best REE Conc in product, %
2	Brayton Point Power Station, MA	432	5.25	1.2
8	SCANA, Williams Station, SC*	682	6.75	1.4
9	Kentucky State University	1219	4.76	3.7

*The Williams ash was used for supplemental experiments after the Go/No-Go Decision; see Section 5.5.

The general procedures for the smelting tests included the following:

- Preparing a sample mixture of ash and prescribed additives – lime, carbon, supplemental metals.
- Loading the ash sample mixture in a crucible (typically of graphite construction).
- Placing the sample crucible in the test furnace.
- Operating the furnace at the prescribed testing conditions to smelt the ash mixture.
- Removing the sample crucible from the furnace and collecting the slag and metal portions produced.
- Analyzing the metal and slag portions for REE and standard metals content.

Similar to other commercial smelting operations, raw ash samples were mixed with additives to enhance the process and promote separation of the molten mixture into distinct slag and reduced metal phases. Lime (CaO) was added at ratios in the range of 30 – 70% by weight of the raw ash. The purpose of lime addition was to reduce the ash melting temperature and to reduce the viscosity and improve flow characteristics of the melt. Carbon (as activated charcoal) was added in excess as the reductant for both iron oxide and the rare earth oxides. Gas emissions from the smelting process are then primarily CO, produced from carbon reacting with the metal oxides. For some cases, supplemental metals (e.g. iron powder) were added at ratios up to 15% by weight of ash for enhancing REE collection in the molten metal phase. However, this would have the undesired effect of diluting the REE concentration in the metal product. Example pictures of ash sample preparations including powders, ash loaded in a crucible, and pressed pellets are presented Figure 6.



Figure 6. Ash sample preparations including (left to right) Brayton Point ash mixture powder, Brayton Point ash mixture in crucible, and pressed pellets of Kentucky State University ash mixture.

Both laboratory-scale plasma and high-temperature electric furnaces were used to heat ash samples to a molten state – in a reducing atmosphere – with the intention of forming separate slag and reduced metal (iron) phases. The plasma furnace was developed at the University of Utah and consisted of a plasma gun located above a reactor chamber setup. A schematic of the system with pictures is provided in Figure 7. The plasma gun nominal maximum power rating is 100 kW. For a smelting test, a sample crucible is placed inside the chamber and surrounded by insulating material (see picture in Figure 7). One sample of about 15 g can be treated at a time using the plasma system. A graphite lid with an opening is placed on top of the sample crucible. The heated carrier gas plume (argon) from the plasma gun directly impinges on the sample through the opening in the lid. The force of the plume is strong enough to blow sample material out of the crucible before smelting can occur. Therefore, the crucible lid served to prevent material blowout as well as splashing losses due to evolution of gases from the chemical reactions. During operation of the plasma gun, high crucible temperatures are reached quickly, and maximum achievable holding times are about one hour. A key disadvantage for the system, though, is that it does not have the capability for direct temperature measurement inside the sample chamber.

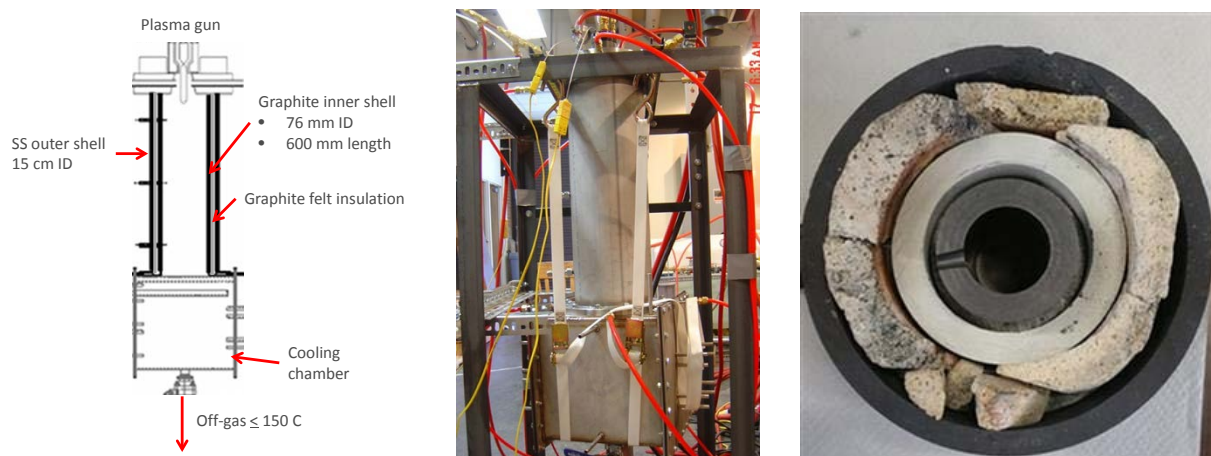


Figure 7. Bench-scale plasma furnace at University of Utah – side view schematic (left) picture of actual equipment (middle), chamber with sample crucible surrounded by insulation (right).

The electric furnace developed by Southern Research (picture in Figure 8) consists of a graphite heating tube element arranged vertically in a water-cooled steel housing, with carbon black insulation between the housing and heating tube. The furnace is powered by a low voltage/high current AC source with variable output control, and the furnace can be heated in excess of 2400°C and held at temperature for several hours. The temperature of the furnace core is measured directly using a thermocouple inserted through a side port in the housing. Optical pyrometry was used to measure temperatures above the operating limit of the thermocouple. The graphite heating tube has an internal diameter of ~90 mm, and the vertical heated zone is ~125 mm. One sample preparation of 30–40 g could be tested at a time. Smelting tests were conducted with a constant helium purge flowing through the furnace to protect the graphite element from exposure to air (O₂) while operating. For a typical test, the sample crucible was loaded, the furnace sealed, and the helium purge was started. Heating then began at a pre-specified ramp rate to a desired hold temperature. Next, the furnace was maintained at the hold temperature for a pre-determined duration, after which, heating was stopped, and the furnace was allowed to cool for safe handling and removal of the sample crucible.



Figure 8. Southern Research electric tube furnace.

After completion of each smelting test, the crucible was removed from the furnace, and the sample was inspected to note the degree of melting achieved. For cases where complete sample melting was achieved, there was a clear separation between metal and slag phases. The slag appeared glassy and the metal formed as shiny nuggets, surrounded by the slag phase. Figure 9 includes pictures of Brayton Point ash samples having distinct metal and slag phases after smelting in an electric furnace.



Figure 9. Crucibles of smelted Brayton Point ash samples with distinct metal and slag phases.

Slag and metal fractions produced during successful tests were recovered from the crucibles for laboratory analysis. Due to – often significant – material losses during the smelting process, final sample weights could not be completely compared against initial weights to close the material balance. Material losses could have been caused by several factors including:

- Material splashing out of the crucible from gas evolution through the melt from reduction reactions.
- Material blown out of the crucible by the force of the plasma plume impinging on the sample.
- Vaporization of some sample mixture components due to high temperature.

The slag and metal fractions were analyzed at the Southern Research analytical lab. Specimens of ~50 mg were first digested in trace metal grade concentrated HF (48%) and Aqua Regia at 105 °C in a hot block until incipient dryness. Any leftover residue was dissolved in a 0.05% HNO₃ solution. Each digestate was then analyzed for REE and standard metals content using ICP-MS (Agilent Technologies Series 7700). Table 5 summarizes test conditions and analytical results for specimens produced during the smelting tests. REE concentrations measured in both the metal and slag portions are provided as well as a theoretical, best-case maximum value for the metal portion – given as µg of elements per g of ash.

Table 5. Summary results of smelting tests.

ID	Sample Mixture	Furnace Used	Smelting Temp, °C	Smelting Time, min	Theoretical Max REE in Metal, µg/g	Total REE in Metal, µg/g	Total REE in Slag, µg/g
-0012	BP/50% lime/14.3% Iron	Electric	1500	180	2404	2.4	214.0
-0014	BP/50% lime/14.3% Iron	Electric	1550	240	2404	0.2	194.3
-0013	BP/50% lime/14.3% Iron	Electric	1550	240	2404	1.3	No Data
-0030	BP/30% lime/10% Iron	Electric	1760	120	3160	0.9	559.1
-0035	BP/30% lime/10% Iron	Electric	~1900	No data	3160	93.8	608.9
-0042	BP/30% lime/10% Iron	Electric	2093/1982	120/120	3160	91.7	172.0
-0044	BP/30% lime/10% Iron	Electric	1927	180	3160	212.3	No Data
-0045	BP/30% lime/10% Iron	Electric	1871	60	3160	50.9	59.1
-0017	BP/50% lime/5.7% Iron	Plasma	No Data	20	4609	29.2	214.3
-0020	BP/50% lime/10% Iron	Plasma	No Data	42	3160	56.9	No Data
-0018	BP/50% lime/10% Iron	Plasma	No Data	60	3160	129.4	294.5
-0049	BP/50% lime/10% Iron	Plasma	No Data	12	3160	14.0	327.3
-0047	BP/50% lime/10% Iron	Plasma	No Data	40	3160	33.5	351.7
-0055	KFC/70% lime/10% Iron	Plasma	No Data	26	9145	11.5	946.0
-0060	KFC/70% lime/10% Iron	Plasma	No Data	33	9145	18.8	221.1
-0058	KFC/70% lime/10% Iron	Plasma	No Data	40	9145	302.1	1261.0
-0062	KFC/50% lime/10% Iron	Plasma	No Data	15	9145	116.2	1338.1
-0067	BP/50% lime	Plasma	No Data	25	11764	54.6	497.8
-0065	BP/50% lime	Plasma	No Data	34	11764	382.4	376.3
-0069	WS/50% lime	Plasma	No Data	24	14445	4.5	541.0
-0071	WS/50% lime/10% Cu	Plasma	No Data	24	4633	1.2	278.0
-0073	WS/50% lime/10% Co	Plasma	No Data	24	4633	25.0	571.1
-0075	WS/50% lime/10% Ni	Plasma	No Data	24	4633	0.2	489.0
-0078	BP/50% lime, w/H ₂ plasma	Plasma	No Data	30	11764	337.2	No Data

In Table 5, the format for “Sample Mixture” description is “feedstock/additive 1/additive 2”, where feedstocks are denoted as follows: BP = Brayton Point Power Station fly ash, KFC = Kentucky State University Fire Clay ash, WS = Williams Station fly ash. The example code “WS/50% lime/10% Cu” is interpreted as follows:

- WS = Williams Station fly ash feedstock
- 50% lime = lime added at 50% wt of ash
- 10% Cu = copper added at 10% wt of ash.

As was reported in the Task 3 – Feasibility Study, the smelting experiments were not successful at concentrating REE in the reduced metal fraction. Numerous testing conditions were investigated, including varying the lime addition ratio, varying the smelting temperature and hold time, addition of supplemental iron and alternative metal collectors (copper, cobalt, and nickel), and use of hydrogen plasma as the reducing agent. Typically though, as indicated in Table 5, the REE remained in the slag phase at concentrations similar to that of the raw feedstock ash.

4.2 Computational Modeling Summary

Feasibility of the vaporization/condensation process option on the reduced metal phase following the smelting process could not be demonstrated experimentally as complete vaporization of the metal phase would require temperatures in excess of 3000 °C for some mixtures. Therefore, feasibility of this advanced option was evaluated through computational modeling. The vaporization process was evaluated for a complex mixture of condensed species using the equilibrium module of Outotec’s chemical reactions and equilibrium software, HSC Chemistry 9.0. Equilibrium calculations were performed using the Gibbs energy minimization method. The equilibrium module was used to predict the major gas species of each metal in the system along with their partial pressures as a function of temperature. From this data, the potential separation of rare earth element species from the major ash components can be determined.

The primary modeling case study considered sequentially vaporizing a reduced metal phase (after removal of the slag phase) at specific temperatures to allow for further REE separation and concentration. Key assumptions for the modeling procedure included that 0.5% of the slag material would remain in the metal layer (either by dissolving in the metal phase or imperfect separation of the metal and slag phases), recovery of iron in the metal layer would be 95%, and conservative recovery of REE into the metal layer would be 50%. The equilibrium system included iron metal and the major ash elements Si, Al, Ca, and S (sulfur dissolves more easily in iron than other elements) as oxides. The most abundant REE in coal ash – La and Ce – were included. Also included were the more valuable and critical REE occurring in coal ash in appreciable amounts – Sc, Y, Nd, Dy, and Yb (ytterbium). Finally argon was included in the equilibrium system as argon plasma would be used to heat the reactor and sweep out the vaporized metals.

All potential gas and condensed compounds that can be formed with the preceding elements that are available in HSC were used. After a careful review, the number of compounds was pared-down by removing duplicates or those for which data is only available at low temperature and do not extrapolate well to high temperatures. Finally, the dominant 1 or 2 gas species for each element were retained as determined by running the system. The final system included 84 condensed species and 15 gas compounds.

A minimum flow of argon would be required to maintain the reactor temperature. However, the flow and temperature can be varied in a plasma torch depending on what is required to carry metal vapors out of the reactor into the collection system at some minimum velocity. After performing several equilibrium

simulations, it was determined that the argon flow should be minimized for the best REE separation. Therefore the total argon used during the vaporization run time was set to be equal to the metal charge in the furnace after smelting (mass basis).

The equilibrium results were evaluated to choose operating temperatures that result in the best separation of REE. Equilibrium was also used to predict the composition of the gases exiting the furnace at each temperature. Example equilibrium simulation results considering vaporization of the metal produced after smelting 1 ton of KFC ash are presented in Figure 10. The chart includes curves for the amount of each metal species in the gas phase – expressed as percent of total moles of the metal element in the system – as a function of temperature. The temperature ranges over which each element vaporizes are quite large, and there is significant overlap among various species. However, by strategically choosing temperatures, the REE can be effectively concentrated in certain fractions.

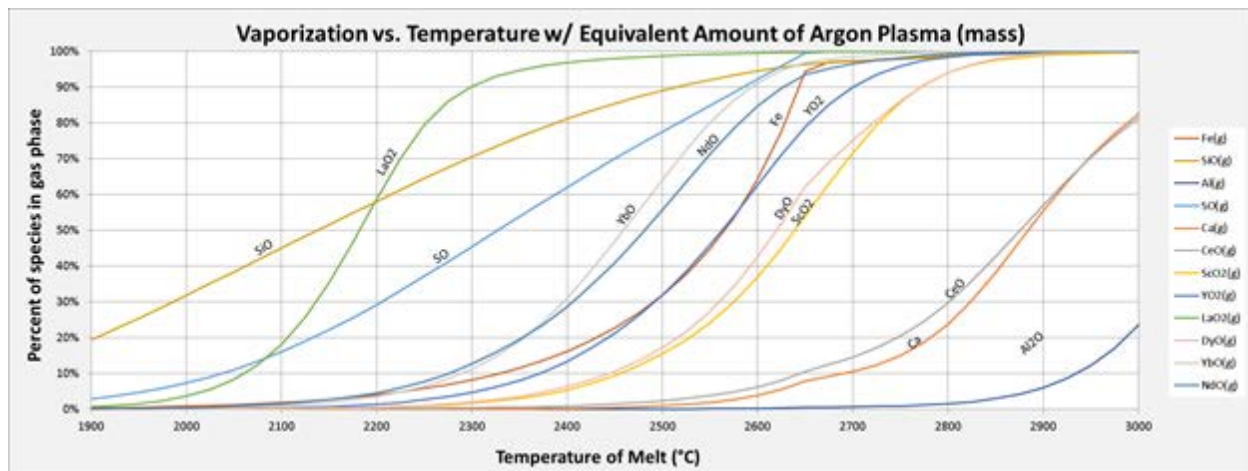


Figure 10. Predicted extent of vaporization of each element as a function of temperature from HSC Equilibrium.

The vapor collection temperatures selected for the system in Figure 10 with resulting product streams are presented in Table 6.

Table 6. Selected vapor collection temperatures and product streams for vaporization/condensation study.

Temperature, °C	Stream	Total REE, %	Description
1925	Initial	0.20	Vaporize as much Si as possible (not collected) before vaporizing first REE
2300	Metal 1	2.81	69% Fe, REE mostly La
2550	Metal 2	1.01	~95% Fe, mixed REE mostly consisting of Nd and Y
2650	Metal 3	0.50	~98% Fe, mixed REE mostly Y and Nd
-	Bottom	4.70	Mix of Fe/Al/Ca, REE mostly Ce with low quantities of Y, Sc, Dy, Nd

From Table 6, the initial operating point is intended to vaporize off as much silicon as possible, and this stream is not collected. All three vaporized and collected metal products are primarily iron with varying REE mixes. Metal 1 REE content is mostly La, Metals 2 and 3 contain lower REE enrichments of mostly Y and Nd, and the bottom metal product is a mixture of Fe, Al, and Ca where the REE content is mostly Ce. Table 7 provides the predicted amount and concentration of each species in each stream assuming an initial feed of 1000 kg of KFC ash to the smelting process.

Table 7. Amount and concentration of each species in each product stream from the vaporization process assuming 1000 kg of feed to the smelting process.

Species	Initial Stream		1 st Metal Product		2 nd Metal Product		3 rd Metal Product		Bottom Product	
	kg	wt%	kg	wt%	kg	wt%	kg	wt%	kg	wt%
Fe	0.1327	22.557	2.4685	68.946	11.5756	94.839	15.6165	98.095	1.8047	38.367
Si	0.2891	49.134	0.6259	17.482	0.2790	2.286	0.0568	0.357	0.0466	0.991
Al	0.0000	0.000	0.0001	0.002	0.0012	0.010	0.0032	0.020	0.8566	18.211
S	0.0003	0.052	0.0035	0.098	0.0033	0.027	0.0012	0.008	0.0000	0.001
Ca	0.0000	0.001	0.0011	0.030	0.0349	0.286	0.1084	0.681	1.7118	36.392
Ce	0.0000	0.003	0.0007	0.020	0.0068	0.056	0.0133	0.084	0.1768	3.759
Sc	0.0000	0.000	0.0004	0.011	0.0051	0.042	0.0068	0.043	0.0105	0.224
Y	0.0000	0.003	0.0045	0.127	0.0398	0.326	0.0317	0.199	0.0204	0.434
La	0.0010	0.163	0.0825	2.304	0.0083	0.068	0.0005	0.003	0.0003	0.006
Nd	0.0002	0.026	0.0110	0.308	0.0519	0.425	0.0196	0.123	0.0058	0.124
Dy	0.0000	0.000	0.0004	0.010	0.0046	0.037	0.0063	0.039	0.0068	0.145
Yb	0.0000	0.001	0.0011	0.031	0.0068	0.056	0.0017	0.010	0.0003	0.007
O	0.1651	28.058	0.3807	10.632	0.1881	1.541	0.0538	0.338	0.0630	1.340
Total	0.5884	100	3.5803	100	12.2055	100	15.9198	100	4.7038	100
Total REEs	0.0012	0.20%	0.1006	2.81%	0.1233	1.01%	0.0798	0.50%	0.2210	4.70%

Per the original concept explored in the Feasibility Study (Task 3), the furnace exit was equipped with a series of collection tubes where the metal vapors would deposit and condense, each tube corresponding to a prescribed vaporization temperature condition in the furnace. The collection tube consists of a generic geometry with internal wall and baffle plate surfaces where vapors exiting the furnace would pass through and deposit. Vapors not condensing and leaving the collection tubes would be treated in the exhaust gas cleanup/scrubbing system prior to final venting.

Computational Fluid Dynamic (CFD) modeling was used to evaluate the effectiveness of the cooled tube in condensing and capturing the metal vapors. The tube was designed to require high gas velocities through the throat area above each baffle with sudden changes in gas direction to allow for smaller particles to escape the gas flow and impact on the walls.

Prior economic calculations were formulated assuming all material collected in a given tube would be combined as a single metal product. However, as vapor pressures vary for each condensing species, some additional separation can occur along the length of the tube. For example, SiO and Al condense in the same general position as REE, but sulfur and calcium condense later at a position further down the tube. The tube, therefore, could potentially be sectioned resulting in collecting a further enriched REE product. The current CFD model assumed that the leading edge of the baffled tube must be cooled quickly as that would be approximately the highest safe operating temperature of any iron based metal alloy. If this temperature could be increased and the cooling rate decreased, there is the potential to also spatially separate REE from Al, Si, and Fe.

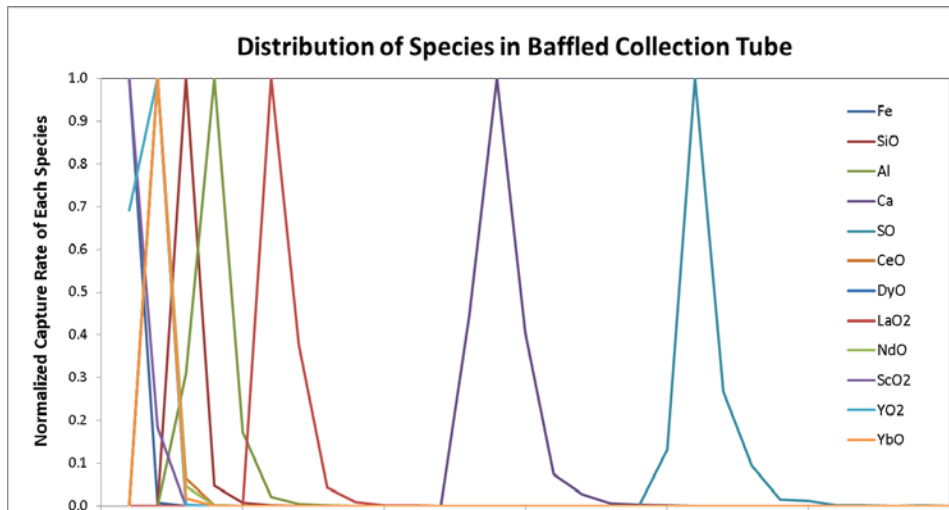


Figure 111. Distribution of the condensed species in the collection tube.

4.3 Economic Analysis

Economic feasibility for a commercial-size REE recovery unit was explored considering an installation contiguous to a hypothetical ~1000 MW-scale coal-fired power plant, having the capacity to process a major portion of the fly ash volume generated by the plant. The capital investment and operating costs were estimated for a unit sized to process 350 metric tons per day (tpd) of raw ash plus any necessary additives (combined total solids of 500 – 550 tpd). The total potential value of products recovered from the fly ash feedstock was determined by including the following:

- Value of the REE concentrated in the smelted metal product.
- Value of a ferrous/titanium metal alloy product.
- Value of the slag phase material, which can be sold, for example, as aggregate for cement production.

Table 8 lists the assumed market prices used for the determining the value of the various metals and products recovered from the fly ash feedstock. The rare earth metal prices reflect averages and projections based on various sources such as Argus Media, Alibaba and Mineralprices.com. Unfortunately, few sources provide reliable REE pricing forecasts, and the data from those available can vary widely. It was also assumed that the recovered rare earth content could be sold as a low-concentration mixture at 50% of their assumed individual pure metal market prices. Considering the total investment, operating costs, and value of recovered products, profitability metrics for the commercial recovery unit were calculated. The chart in Figure 12 includes plots of payback period in years and the return on investment (ROI %) vs. recovery value in \$/ton of raw ash processed by the unit. For example, a payback period of ~5 years with 30% ROI could be realized for a recovery value of \$325/ton of raw ash. For the assumed product prices, such value could be achieved with 80% REE content recovery from the Kentucky State University ash feedstock.

Table 8. Prices assumed for various metals and products recovered from coal ash feedstock.

Element	Purity	Assumed Price, \$/kg
Sc Metal	99.90%	\$15000
La Metal	>99%	\$7
Ce Metal	>99%	\$7
Pr Metal	>99%	\$85
Nd Metal	>99.5%	\$100
Sm Metal	>99.9%	\$10
Eu Metal	>99.5%	\$1000
Gd Metal	>99%	\$60
Tb Metal	>99.9%	\$1000
Dy Metal	>99%	\$400
Ho Metal	99.9 – 99.99%	\$650
Er Metal	99.9 – 99.99%	\$100
Tm Metal	99.9 – 99.99%	\$1000
Yb Metal	99.9 – 99.99%	\$300
Lu Metal	>99.99%	\$2000
Y Metal	>99.9%	\$50
Pig Iron	-	\$0.33
Ferro-Titanium	Ti (30%)	\$3.30
Aggregate slag product	-	\$0.02

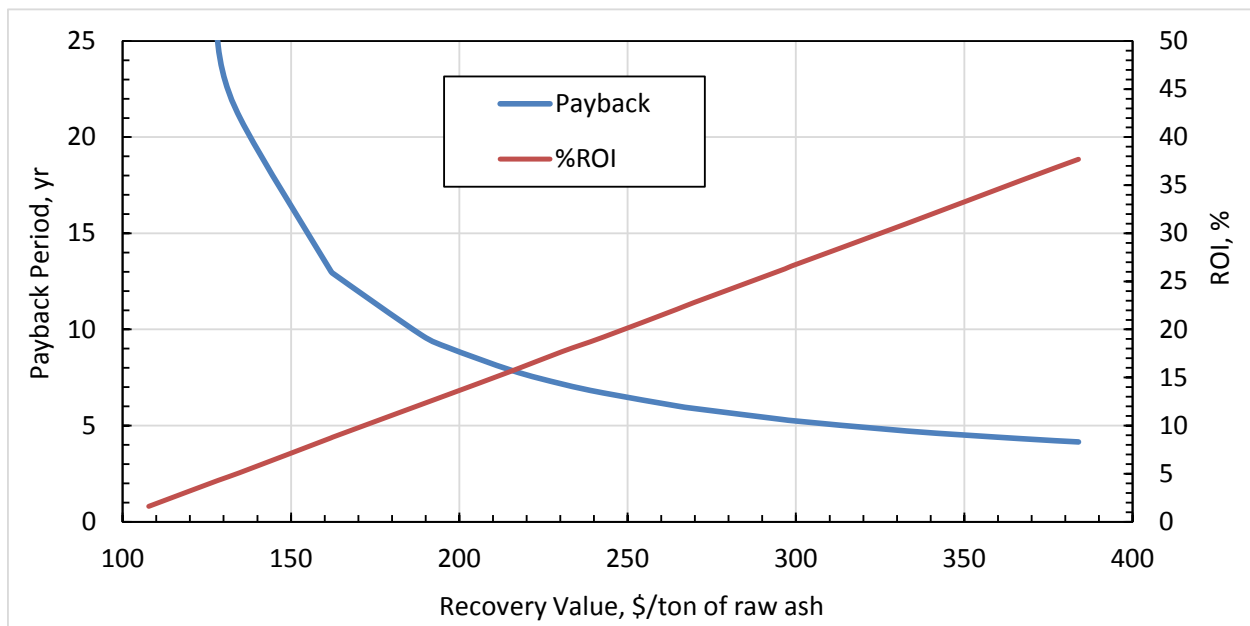


Figure 122. Payback period and ROI vs potential recovered value per ton of coal ash feedstock processed.

5. TECHNOLOGY REASSESSMENT

As noted in Section 4, the bench-scale ash smelting experiments demonstrated the ability to separate coal ash into slag and metal portions. However, the originally proposed technology concept has not been fully proven as only low REE concentrations in the metal phase (few 100 ppm) had been achieved experimentally by the time of the *Go/No-Go* decision point. Typically, the REE components remained in the slag phase at concentrations similar to that of the raw ash feedstock. The subsequent key elements of the project – developing the vaporization/condensation process option and preparing a design package for a pilot-scale demonstration unit – are dependent on a viable smelting process, which performs as originally conceived. Therefore, during the second half of the project, the effort focused on determining how to improve the smelting process for achieving higher REE recoveries and concentrations in products, and this section summarizes those findings.

5.1 Review of Fundamentals

Few naturally occurring ores are known to contain REE in concentrations more than 1% – Monazite is one example – which is evidence that REE lack chemical properties that allow them to be selectively extracted from melts and mixtures. One of the few distinguishing physical properties is their strong bonding with oxygen to create stable oxides (more stable than SiO_2 and Al_2O_3), which is quantified by the Ellingham diagram, presented in Figure 13. The figure shows that as the equilibrium partial pressure of O_2 (p_{O_2}) is sequentially reduced (O_2 is removed from the system) REE will be last to give up their oxygen and be reduced to metals (more negative ΔG_f° values in Figure 13).

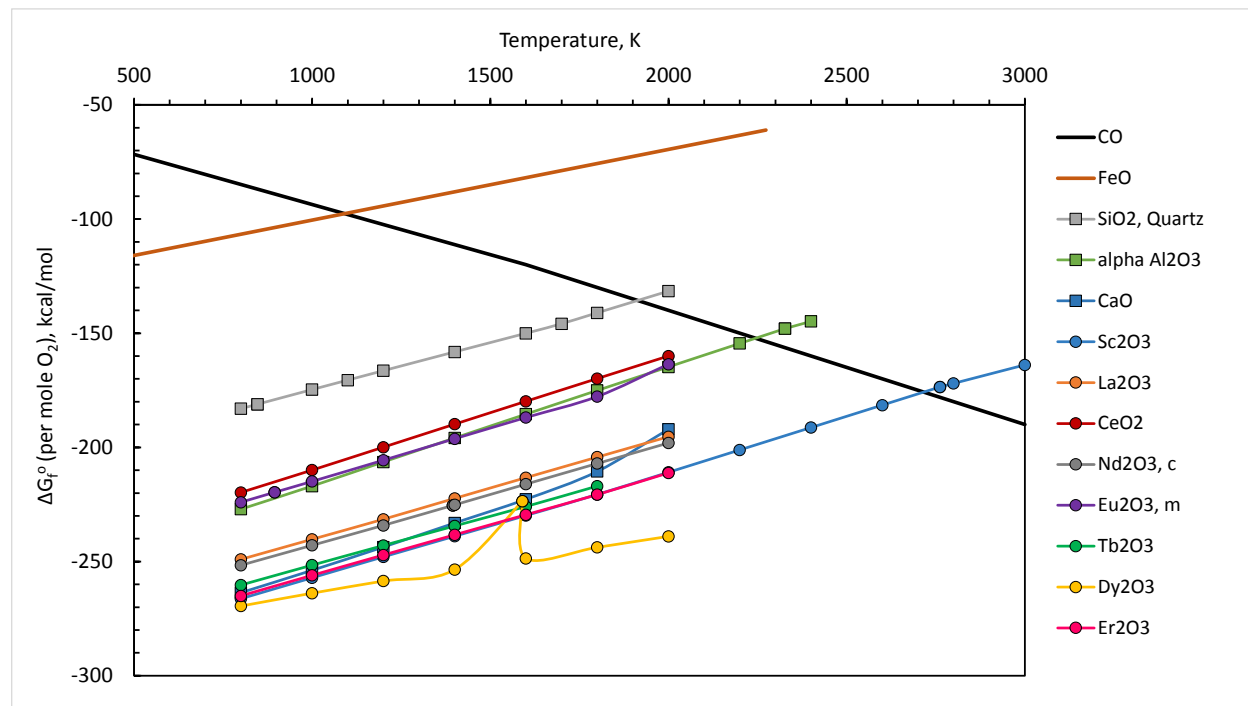


Figure 133. Ellingham diagram (per mole O_2 basis) for select REE and metal species.

According to the originally proposed concept, as the melt was reduced (p_{O_2} lowered) then metallic iron would be released from the slag phase and act as a collector for reduced REE. The position of the curves on the Ellingham diagram indicate that this is unlikely – iron oxide is located near the top of the diagram and is reduced more readily while the REE curves are located near the bottom. For the original concept to

be valid there would need to be some unusually stable compounds with iron (high melting point alloys). The concept has been refuted by the bench-scale experimental results, where, as noted, the REE were found to mostly remain in the slag phase. REE strong affinity for oxygen may be a reason why they are so diffuse in nature: because they bind strongly to oxygen and remain in the vitreous phase as mixed oxides. The application of a “collector phase” may still be possible for REE, but more likely would be for a compound whose curve is located much lower down on the Ellingham diagram.

5.2 Review of Related Applications

The conventional ways to extract REE from industrial wastes are based mainly on hydrometallurgical treatments. However, large amounts of water and chemicals are required for such treatments, which calls into question the future sustainability of these processes. Today, processes based primarily on high temperature pyrometallurgical treatments are attracting more attention for their better environmental impact (Tang et al., 2014). Existing state-of-the-art technologies for recycling of precious and other metals from industrial wastes are now based on high temperature smelting processes using Pb, Cu, and Ni as collectors for the high-value metals. However, the smelting flow sheets are not fully developed yet for REE recovery, as they revert to the oxide phase (slags or fluxes) in a diluted form. In all experiments almost all REE (~99%) go to the oxide phase. However, the key issue remains to get the pyrometallurgical recycling process to concentrate the REE in the original product(s).

Pyrometallurgical techniques have been used for recovering metals from waste streams for more than 2 decades but there has been a lack of development in extracting REE from those wastes. Unfortunately, most processes use oxidizing techniques that cause most critical elements and REE to end up in the slag of smelters or in landfills. A major issue for REE has been unstable pricing and lack of pyrometallurgical experimentation which have been barriers for widespread application of these technologies.

There are three areas where pyrometallurgical processes are starting to be effectively used for the concentration and extraction of REE: 1) the recovery of REE from rare-earth (Nd-Fe-B) permanent magnets, 2) the recycling of REE from nickel metal hydride rechargeable batteries, and 3) recovery from bauxite residue (red-mud).

Recently companies have developed pyrometallurgical flow-sheets for the recycling of valuable metals from rare earth permanent magnets (REPMs), which account for more than 26% of the worldwide consumption of REE, and the stock of redundant material is present in the electronic goods using these magnets. The actual source of the REE is the residue generated at the final finishing stage of manufacturing (swarf), small magnets in end-of-life consumer products, and large magnets that are found in hybrid cars and wind turbines. REPMs typical REE composition is Nd, Tb, Dy, and Pr, all critical rare earth metals. Use of pyrometallurgical techniques have been developed as an alternative to hydrometallurgical routes to simplify the steps involved, reduce the use of large amounts of chemicals and water, and reduce the considerable energy expended over long processing times. The thermodynamics of REPM extraction are based on the Fe-Nd-B alloy phase diagram. With 10-20 g of Nd-Fe-B in every hard disk drive and because these drives are the most important source of REE scrap, the Nd-Fe-B system has been studied to understand the behavior of the metal alloy under high temperatures and then applied to pyrometallurgical recycling for REE extraction and refining (Firdaus, Rhamdhani, Durandet, Rankin, & McGregor, 2016; Hallemans, Wollants, & Roos, 1995).

While a number of multi-stage techniques have been developed for recovery of REE from magnet waste by high-temperature processing, they are still at the research stage, with none yet applied at a commercial

scale in industry. However, more options are available using a combination of pyrometallurgy and hydrometallurgy than with just hydrometallurgy, since both the alloying metal and/or the REE metal can be produced, depending on the technique used. The appeal of all the techniques is based on the strong affinity of oxygen to REE. In extraction recycling for REPM or for other industrial waste streams, which could include coal ash, REE are usually extracted in forms of oxide, halide, fluoride, and other metallic compounds to then be further reduced to metallic form. The intermediate compounds can also be used as an extractant, or to accommodate the extraction process itself.

Another area of promise is the recycling of valuable metals from batteries, which can produce a slag relatively rich in rare earths. In 2011 Rhodia (Solvay) and Umicore announced a jointly developed process for recycling rare earths from NiMH batteries (and lithium batteries). The process is proprietary but is based on Umicore's patented Ultra High Temperature (UHT) smelting process. What is known is that the batteries are fed into a vertical shaft furnace together with coke and a slag. Oxygen enriched air is injected and the metals are converted into a Ni-Co-Cu-Fe alloy and a slag. The slag contains oxides of Ca, Al, Si, and Fe, but also contains lithium and rare earths. The oxide slags are processed to recover the lithium and to make rare earth concentrates processed at Solvay's REE separation plant in France, which uses a hydrometallurgical process (Verhaeghe et al., 2011).

One last area to note involves research on REE extraction from bauxite residue, which currently finds no major industrial application, but is most similar to coal ash in chemical composition and initial REE concentration. During alumina production from bauxite using the Bayer process, rare earths end up in the waste slurry known as red mud, which is rich in iron oxide. Some red muds have been found to contain REE in the range of 1000–2500 ppm with Sc, Y, La, Ce, and Nd being the most prevalent. Recovery of metals from red mud could be economically feasible with suitable extraction processes. Recent approaches have advanced what is called "complex processing" which includes pyrometallurgical treatments to first separate and recover the iron fraction, leaving the REE concentrated in the remaining slag phase (Borra, Blanpain, Pontikes, Binnemans, & Van Gerven, 2016a, 2016b; Loginova, Kyrchikov, Lebedev, & Ordon, 2013). Hydrometallurgical treatments are then proposed to recover REE from the slag.

From review of thermodynamic data and developed (or developing) applications of REE recovery from other industrial waste streams, the affinity of REE for slag phases seems well established. It is likely, then, that such consideration should also be given to recovery processes for extracting REE from coal fly ash. Though pyrometallurgical separation techniques have been shown to be useful in other applications, further study and development are needed for determining the appropriate conditions for such treatment of coal ash and whether rare earth oxide concentration in slag is the preferred route to follow.

5.3 Supplemental Modeling

Reaction Engineering (REI) explored the technical feasibility of partial separation of REE from coal ash by sequentially extracting carbothermally reduced ash metals followed by a sequential volatilization and condensation process. The process was evaluated for a complex mixture of condensed species using the equilibrium module of Outotec's chemical reactions and equilibrium software, HSC Chemistry 9.0. Equilibrium calculations are done using the Gibbs energy minimization method. For a commercial installation, argon plasma was chosen to keep the reactor headspace hot and to sweep out vaporized metal. Therefore a series of equilibrium calculations were made to simulate this transient process.

Recovery of metal vapor from the gases exiting the vaporization reactor and evaluation of additional separation due to differences in dew-point temperatures presented a challenge that was investigated

with CFD modeling. The cooled baffled, collection tube (described in Section 4.2) was utilized to capture condensing vapor exiting the reactor. As gases cool in this tube, some condensation occurs on tube surfaces, but the majority of the metal will nucleate into tiny particles that can grow primarily by particle coagulation. The baffled tube design has small throat cross-sections above each baffle through which gases must accelerate to very high velocities resulting in penetration back to the next baffle before abrupt changes in direction. Thus much smaller particles have enough momentum to exit the gas flow and impinge onto walls than is seen in more traditional cyclone collection systems.

REI's CFD model for multi-phase reacting flows (GLACIER) was utilized for the Task 3 Feasibility Study, but required several additions. GLACIER has been used to model hundreds of industrial systems fired with a broad range of fuels. The code includes models to track particle trajectories and surface deposition due to impaction, thermophoretic forces, and Brownian motion. Due to the very small sizes of particles, particle deposition (capture) was predicted based on microscopic forces (e.g., van der Waals and/or electrostatic forces). At the beginning of the project, GLACIER did not contain a condensation, nucleation, or particle coagulation and growth model. A simple condensation routine and particle coagulation model was incorporated prior to the Feasibility report.

In the simple condensation routine, partial pressure of each gas species were compared against vapor pressures that are input independently per HSC calculations. As the gas temperature drops, the vapor pressure eventually falls below the partial pressure and condensation occurs at a rate required for equilibration. In dilute flow systems, nucleation of fine fume particles dominates wall condensation, thus it was assumed that all condensing gases form ~3 nm size particles. Due to complications of incorporating this routine into a CFD framework with continuous nucleation of new condensed fume particles, this routine was previously only incorporated at each baffle location. The coagulation model of MAEROS 2 was utilized to predict particle growth before the next baffle and Glacier models deposition onto wall surfaces.

Development work has now been completed on a more physically accurate model of the particle formation and growth mechanisms. Previous implementations of MAEROS 2 into the CFD framework only included the particle coagulation module. The nucleation and coagulation models were specific to water species and only worked over a narrow range of low-temperature applications. These modules were upgraded by REI using more robust algorithms and included a capability for modeling the processes for all major ash inorganic and REE species. Nucleation of particles and growth by both coagulation and surface condensation are both now modeled as a continuous process in the modeling domain.

The process was evaluated for a complex mixture of condensed species using the equilibrium module of Outotec's chemical reactions and equilibrium software, HSC Chemistry 9.0. All major ash species (Si, Al, Ti, Ca, Fe, K, Mg, Na, S, and P), target REE species (Ce, Dy, La, Nd, Sc, Y, and Yb), and carbon as a reductant were included in these simulations. The total number of both gas and condensed compounds available in HSC 9.0 included over 1000 compounds. This list was pared down to just under 200 compounds based on metallurgical knowledge and experience to eliminate compounds with unreliable data, duplicates, and physically unrealistic compounds.

Several simulations were completed for varying amounts of added carbon. It was discovered that the use of carbon to reduce the major ash species was necessary to lower the vaporization temperature of these species. However if too much carbon is added, refractory-like metal silicates and carbides form that are stable up to extreme temperatures. Even though oxygen combines with carbon and is primarily evolved as CO, it was discovered that the amount of carbon needed for complete reduction of the ash species to CO was too much. Instead carbon was added at a rate necessary for complete reduction of ash and oxide

conversion to CO₂ (17.9% of ash by weight for Williams Station ash). Oxygen still evolved primarily as CO and some ash species were only partially reduced, but carbide formation was avoided.

For comparison with supplemental experiments (see Section 5.5), the simulations were based on the Williams Station fly ash composition, having total REE content of 682 ppm with the 7 target REE included in the simulation totaling 591 ppm. The results of the initial HSC equilibrium simulation are displayed in Figure 14, with the major gas species for each metal shown on the graph.

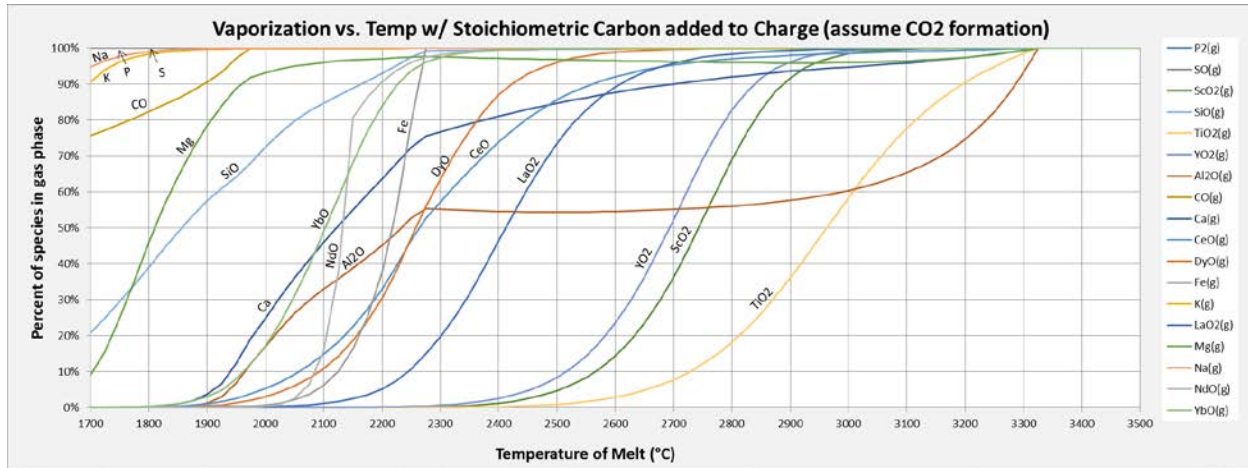


Figure 144. Predicted extent of vaporization of each element as a function of temperature based on HSC equilibrium simulations of carbothermic ash reduction and vaporization.

The first step is to reduce and remove as much of the major ash species as possible while minimizing the vaporization of REE. A temperature of 1800°C was chosen for this first step. Figure 14 displays the vapor-liquid equilibrium prediction of a closed system. However, gases are allowed to exit the top of the reactor and argon plasma is used in the headspace to keep the reactor hot and sweep the vaporized species out the exit. As the metal vapor is removed, more metal will vaporize to attempt to maintain equilibrium. Thus the composition and predicted vapor pressure changes with time. A series of equilibrium simulations were performed with the melt composition updated as species were removed through vaporization.

In the initial equilibrium, <0.5% of any single REE component vaporized. Holding the reactor at this temperature for longer periods, however, results in loss of more REE with time. Through optimization of the hold time, 62% of the ash/carbon mixture can be removed through vaporization with only a loss of 0.7% of the REE. As the REE content of this metal vapor is <6ppm, there will be no effort to recover the REE from this stream. The total REE content in the ash/carbon melt is increased from 501 ppm to 1314 ppm in this initial step.

Figure 15 displays the updated vaporization curves of the primary gas compound for each species based on the HSC equilibrium calculations after removal of the material vaporized in the initial step. Yttrium and Scandium are highly refractory and will remain in the melt up to high temperatures. However the vaporization extent of the other target REE species is similar to the major ash species still remaining, except for titanium. However there is a significant break between Yb and Dy. The goal of the next step is to further remove as much of the major ash species, while keeping Dy, Ce, La, Y, and Sc in the melt. Therefore, it was decided that the next step should be to increase and hold the reactor temperature at 2100°C.

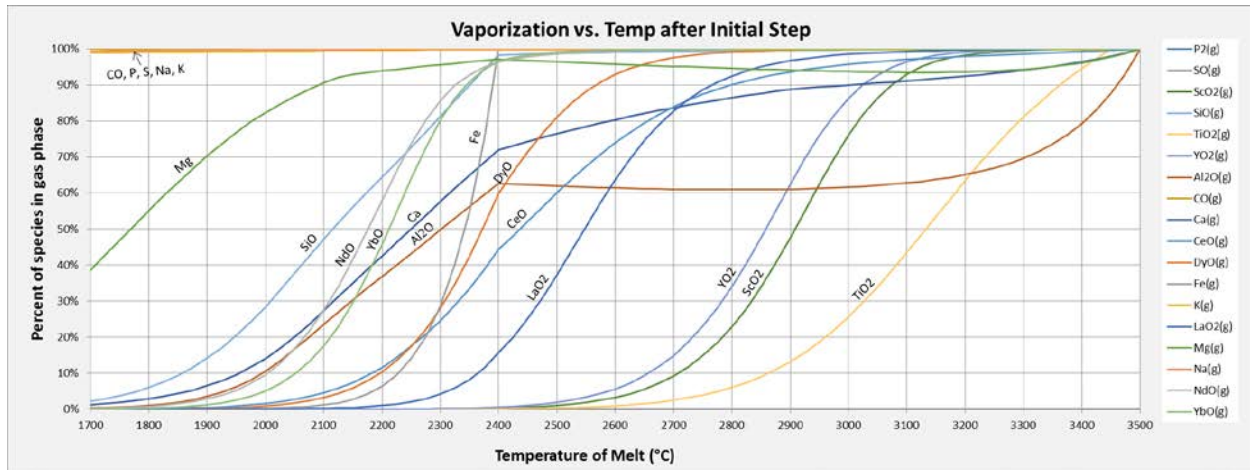


Figure 15. Predicted extent of vaporization of each element as a function of temperature based on HSC Equilibrium simulations of carbothermic ash reduction and vaporization for step 2.

By optimizing the hold time based on a series of equilibrium predictions, the melt weight is reduced by another 20% to only 17.4% of the initial mass of the reactor charge. The REE concentration in this melt will increase to >2200 ppm. The concentration of REE in the vapor is 520 ppm, consisting primarily of 82% and 60% of the initial amount of Nd and Yb, respectively. This vapor will condense in the cooled baffled collection tube with potential partial separation, spatially.

The final step is to separate the remaining REE from the more refractory ash species, Ti and Al. Figure 16 displays the updated vaporization curves of the primary gas compound for each species based on the HSC equilibrium module after removal of the material vaporized in step 2. It is possible to perform 2 steps where La, Dy, and Ce are first collected and then Y and Sc are collected at a higher temperature step. However for this simulation, these REE were collected in a single step. Multiple simulations were run between 2750 and 2900°C. Energy requirements and costs increase with increasing reactor temperature, and it was concluded that there is no benefit in running these experiments above 2750°C.

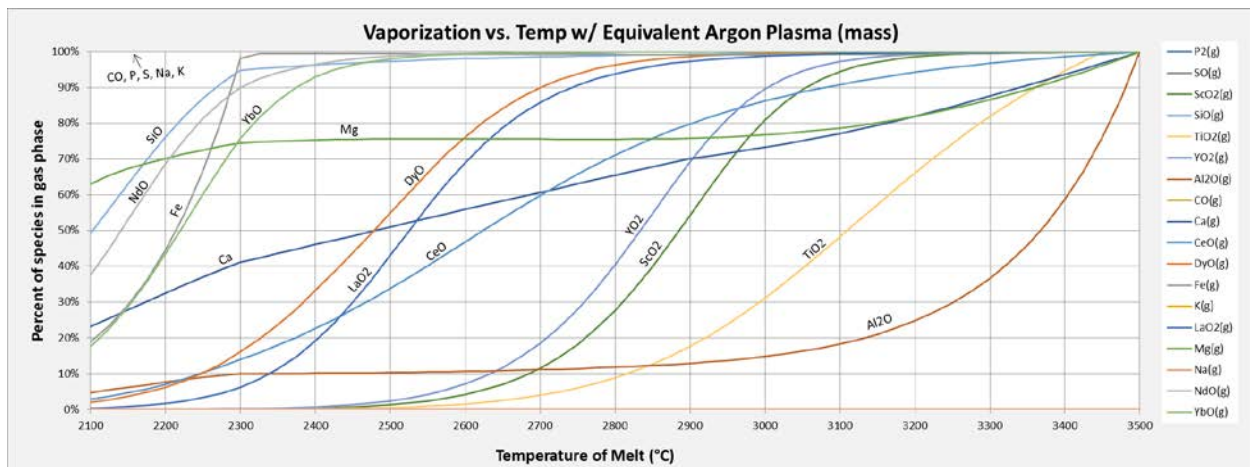


Figure 16. Predicted extent of vaporization of each element as a function of temperature based on HSC Equilibrium simulations of carbothermic ash reduction and vaporization for step 3.

By optimizing the hold time based on a series of equilibrium predictions, the majority of the REE can be vaporized off, while 12% of the initial ash/carbon melt remains in the reactor. Total REE concentration in

the condensable metal portion of the vapor is increased to >7000 ppm, while unrecoverable REE concentration in the melt is <45 ppm.

Table 9 reports the total mass and mass fraction of each component in the resulting product streams with the major REE species in each stream highlighted. Metal product stream 2 contains the highest concentration of REE and is primarily composed of Ce, Dy, La, Sc, and Y. While the total REE content metal product stream 1 is similar to that of the raw ash, the REE are primarily Nd and Yb and are 2.5–3.5 times more concentrated than in the original ash.

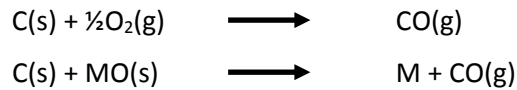
Table 9 Amount and concentration of each species in each stream from the vaporization reactor assuming 1000 kg of ash fed to the reactor with addition of carbon at 17.9% of ash weight.

Species	Initial Product		1 st Metal Product		2 nd Metal Product		Bottom Product	
	kg	wt%	kg	wt%	kg	wt%	kg	wt%
Al	5.7934	1.857	67.0413	27.814	8.2643	12.974	68.1698	67.131
Ca	3.3570	1.076	19.4750	8.080	4.5995	7.221	0.4603	0.453
Fe	0.1235	0.040	14.2697	5.920	33.0934	51.954	0.0000	0.000
K	19.1211	6.130	0.0000	0.000	0.0000	0.000	0.0001	0.000
Mg	5.0814	1.629	0.0743	0.031	0.0000	0.000	0.0000	0.000
Na	2.6117	0.837	0.0000	0.000	0.0000	0.000	0.0000	0.000
Si	174.6355	55.986	76.5475	31.758	6.0002	9.420	0.0000	0.000
Ti	0.0000	0.000	0.0003	0.000	3.1803	4.993	7.6102	7.494
Ce	0.0022	0.001	0.0381	0.016	0.1740	0.273	0.0030	0.003
Dy	0.0001	0.000	0.0025	0.001	0.0170	0.027	0.0000	0.000
La	0.0000	0.000	0.0015	0.001	0.1082	0.170	0.0000	0.000
Nd	0.0018	0.001	0.0772	0.032	0.0150	0.023	0.0000	0.000
Sc	0.0000	0.000	0.0000	0.000	0.0358	0.056	0.0029	0.003
Y	0.0000	0.000	0.0000	0.000	0.1012	0.159	0.0002	0.000
Yb	0.0002	0.000	0.0061	0.003	0.0038	0.006	0.0000	0.000
O	101.2006	32.444	63.4967	26.344	8.1047	12.724	25.3011	24.915
Total	311.9285	100	241.0302	100	63.6975	100	101.5477	100
Total REE	0.0043	0.001%	0.1255	0.052%	0.4551	0.714%	0.0062	0.006%

In the Task 3 Feasibility Study, the use of hydrogen plasma was recommended for further study, noting that atomic hydrogen is a better reductant than carbon, while molecular hydrogen (H₂) is a poor reductant (Sabat, Mishra, & Rajput, 2014). If hydrogen plasma is allowed to impinge upon the surface of an ash melt, it is possible that hydrogen atoms will react with the ash before combining into molecular hydrogen. Supplemental smelting experiments were performed in the plasma furnace using hydrogen plasma with limited success (see results in Table 5). Also, supplemental modeling efforts were performed using the HSC equilibrium module. Unfortunately, molecular hydrogen is thermodynamically stable up to 3500°C, and the amount of hydrogen ion in equilibrium is not sufficient to cause any noticeable reduction of the ash. Therefore it is not appropriate to use equilibrium modeling for this study. Instead an advanced model that includes kinetics of the reaction of hydrogen ions with itself and major ash species would be necessary for this modeling study. Unfortunately, such kinetic modeling tools were not available to the project team.

5.4 Adjustments to Proposed Technology

From review of thermodynamic data, equilibrium modeling of the vaporization process, the first-year experimental results, and other REE recovery applications, the technology approach shifted to an overall strategy of sequentially reducing the ash oxides and removing them from the system one-by-one as metals, leaving behind the REE as oxides, more concentrated in the remaining slag phase. Related to the original ash smelting concept, removal of metals is achieved by carbothermic reduction per the following forward reactions



where M is an arbitrary metal. The reaction becomes more favorable at high temperature because more gas (more entropy) is generated. As noted, carbothermic reduction is common place in many industrial processes, though not at extreme temperatures.

HSC Chemistry was again employed to assist determination of appropriate levels of carbon to use for reducing as many ash oxides to metals as possible while avoiding formation of undesired carbides. At levels closely matching the composition of the Williams Station ash, the following elements were input to the model as oxides: Si, Al, Fe, S, Ca, Na, Mg, K, P, Ti, Sr, and Ba. Only four REE species were input into the system – Y, Sc, La, Dy – because the thermodynamic data for REE was, generally, too sparse to be reliable. La and Y have the most complete thermodynamic properties, and it was assumed these would represent the light and heavy REE, respectively, well-enough for the system. Therefore, all quantitative results for REE concentrations were based on La and Y. The mixture of species was modeled as separate phases (gas, oxide, carbide, phosphide, sulfide, pure metal) where each phase was treated as an ideal mixture of compounds. The key modeling assumptions were 1) thermochemical equilibrium, 2) an ideal mixture, and 3) completely separate phases, though in reality one phase is soluble in another – for example, carbon (carbide) is significantly soluble in molten iron (pure metal).

Resulting equilibrium plots for Si and Al species versus the mole ratio of added carbon are presented in Figure 17 and Figure 18, respectively. Figure 17 shows a SiO peak for an added carbon mole ratio of 0.73, though there is still a high concentration of Al₂O₃ per Figure 18. Figure 19 includes plots of La and Y

recovery yield and the concentration factor $\frac{x_{REE \text{ in slag}}}{x_{REE \text{ in Ash}}}$ – the ratio of the mole fraction of REE in slag to

the mole fraction of REE in the ash sample – versus the carbon addition ratio. Higher carbon additions result in a larger concentration factor but less yield as more REE go to the pure metal or gaseous phase. Results suggest that concentration factors of 20–400 are possible, which for ash with 1000 ppm of REE initially would equate to a 2–40% concentration in the final product with perfect separation of the slag phase. Optimizing the process with regard to carbon addition, considering the trade-off between recovery yield and concentration factor, would involve further economic evaluation on the value of potential products recovered.

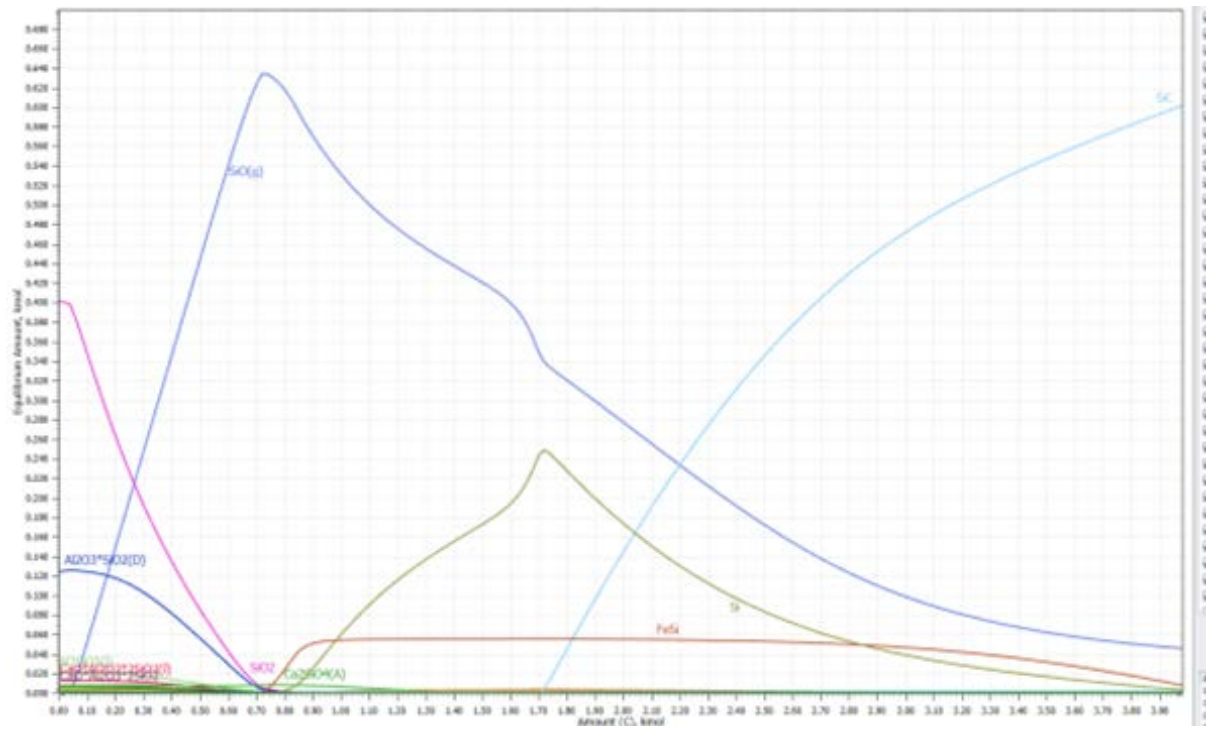


Figure 17. Equilibrium silicon species versus carbon addition at 2200 °C.

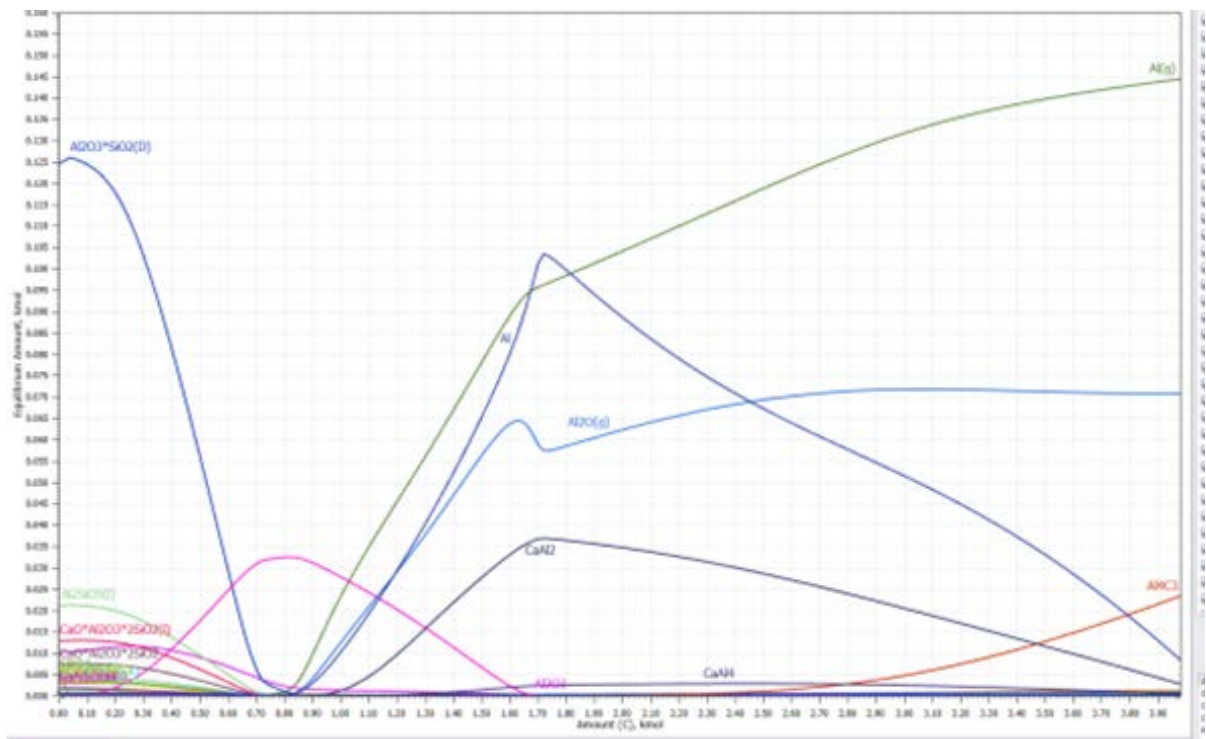


Figure 18. Equilibrium aluminum species versus carbon addition at 2200 °C.

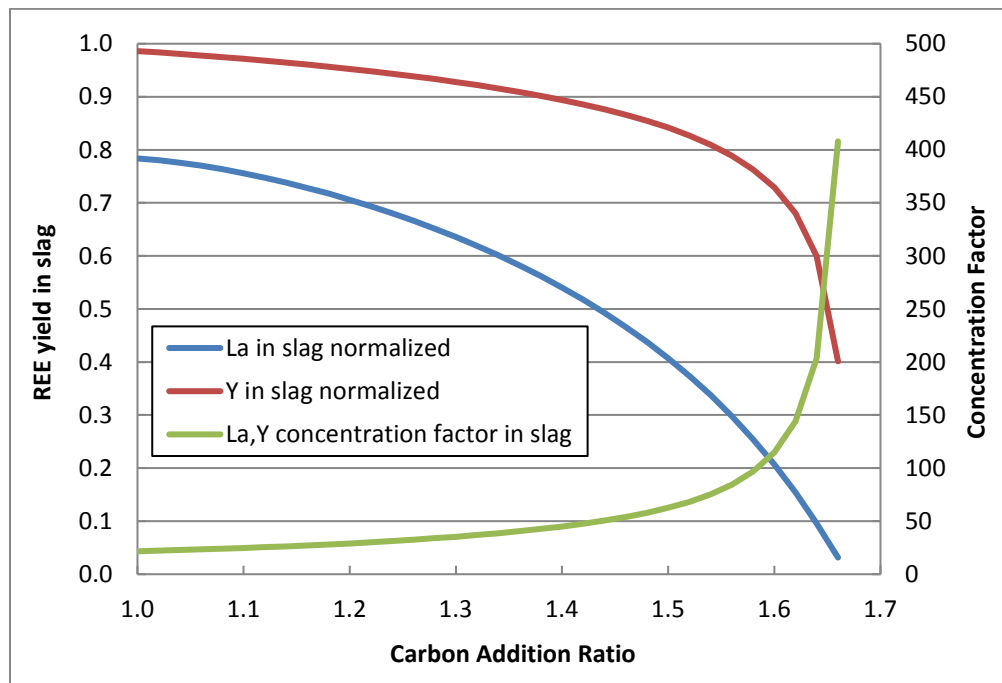


Figure 19. REE recovery yield and concentration in slag versus carbon addition ratio.

5.5 Supplemental Experiments

Supplemental experiments were planned to validate the adjusted smelting process. The tests were performed in the high-temperature electric furnace, which allowed for close monitoring and accurate control of the temperature condition. To prevent splattering and loss of material from the sample crucible as a result of fast and violent gas evolution from the reduction reactions, the temperature was ramped up slowly over several hours to a target temperature of 2200 °C. The system was then held at temperature for two hours to maximize diffusion of species through the melt.

The sample mixtures and results for the supplemental tests are presented in Table 10 including starting REE concentrations, starting and final sample weights, theoretical best and actual REE concentrations in the final products, and recovery yield.

Table 10. Sample preparations and results for the supplemental tests conducted at highly reducing conditions.

Sample ID	Sample Mixture	REE in Mixture, ug/g	Starting Sample wt, g	Final wt, g	Theoretical Best REE in Product, ug/g	Actual REE in Product, ug/g	Recovery Yield, %
Test 8*	KFC/30% SiO ₂ /50% lime/10% iron	531	27.616	6.7	2189	908	41.5
Test 9	WS/30% iron/19.6% C	456	32.599	9.81	1515	457	30.2
Test 10	WS/15% lime/30% iron/42.1% C	365	31.404	9.576	1195	608	50.8

*Test 8 was performed with a lower carbon ratio (stoichiometric with Fe₂O₃ content) and smelting temperature (1954°C), but results and the residual product resembled those of Tests 9 and 10.

Rather than producing distinct slag and metal phases, these experiments each produced reduced Si-Al-Fe intermetallic residuals having final weights about 25-30% that of the starting sample weights – Figure 20 includes pictures of the residual at the bottom of each crucible from Tests 9 and 10. With further inspection, the residual products had a shiny yet grainy appearance. The material was brittle and easy to fracture with a scribing tool.



Figure 20. Residual products from Tests 9 and 10.

From Table 10, Tests 8 and 10 were successful to concentrate REE in the product as compared to the starting sample – concentration factor of 1.7. However, much of the REE content was lost (likely to vaporization) as recovery yields were in the range of 30–50%.

To further evaluate the structure and composition of the residual products, specimens from Tests 9 and 10 were analyzed using Scanning Electron Microscopy – Energy Dispersive Spectroscopy (SEM-EDS). Small sections, having residual material attached, were cut from the bottom of each crucible. These were then mounted in epoxy and polished. Figure 21 is a picture of an example polished, epoxy-mounted specimen for SEM-EDS analysis.



Figure 21. Example epoxy-mounted SEM-EDS specimen.

Using SEM, points of REE accumulation in the specimen were located by inspecting backscattered electron (BSE) images. Figure 22 is an example of a SEM BSE image taken from the Test 10 residual specimen, having bright, “white” areas, circled in red, which indicate regions of heavy element (high atomic number) content. Figure 22 includes a view at the 100 μm length-scale and magnified views of the circled areas to the 10 μm length-scale.

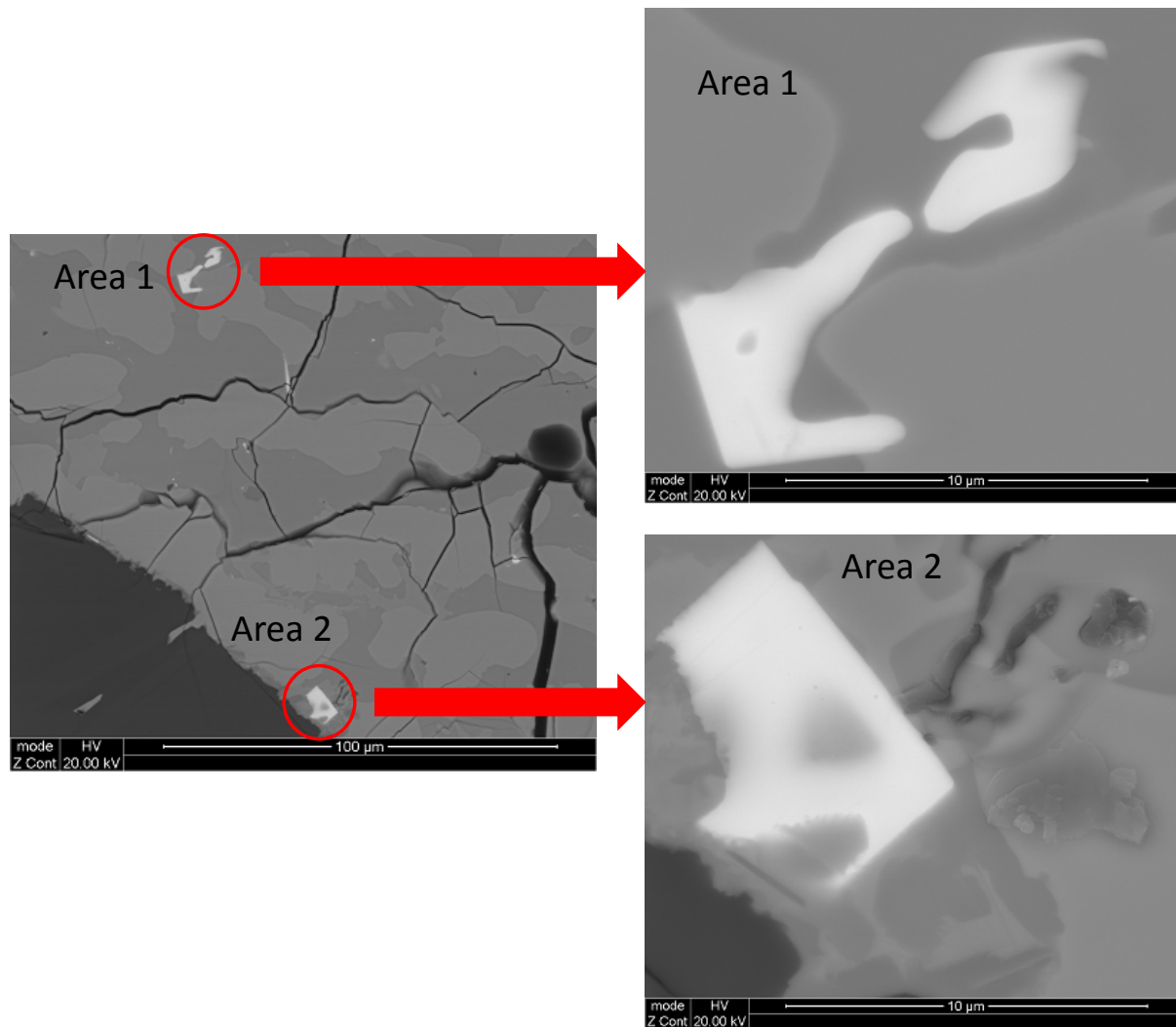


Figure 22. Example SEM images containing regions of REE accumulation indicated by the bright, white areas – Areas 1 and 2 circled in red. The view on the left is at the 100 μm length-scale while the right images are magnified views to the 10 μm length-scale for Area 1 and Area 2.

Areas 1 and 2 were analyzed for composition and were verified to be localized regions of high REE concentration. An example spectrum for the bright region of Area 2 (Figure 22) is presented in Figure 26, which contains several distinct REE peaks including Ce, La, Nd, and Y, which is consistent with the feedstock characterization results as these were the more abundant REE detected (see Section 3). Table 11 includes the tabular analytical results for the peaks in the Figure 23 spectrum including weight %, atomic %, intensity, and error. Combined, the REE content of the bright Area 2 amounts to 28.5% (by weight). Similarly, Area 1 was also found to contain a high weight fraction of REE near 40%. Oxygen content in the white regions was found to be quite small, which seems to indicate that the smelting process succeeded in reducing the REE oxide content in the raw ash to metal form in the residual product.

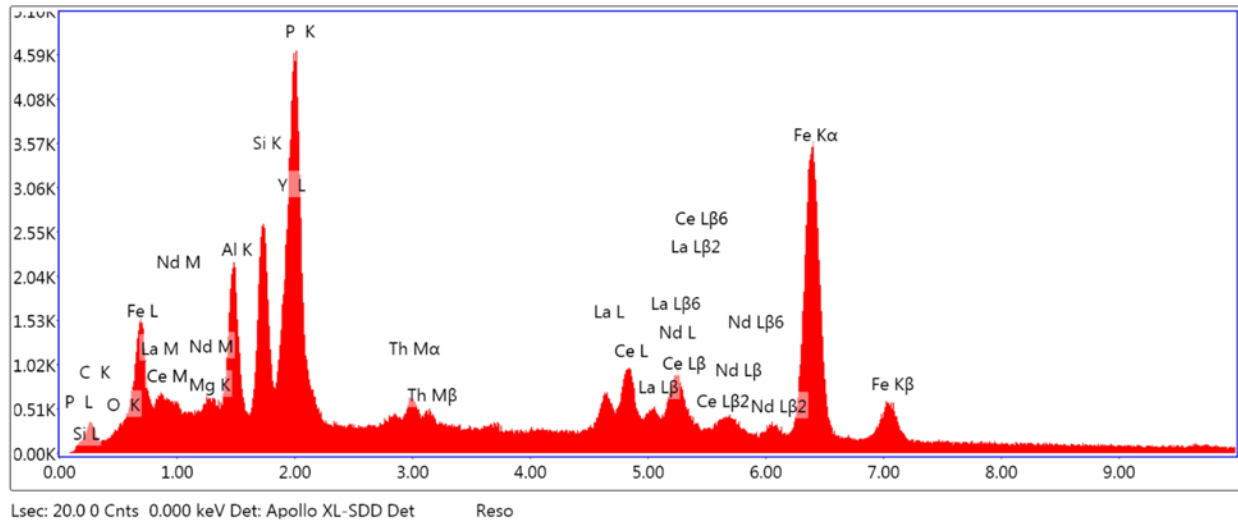


Figure 23. Example spectrum for the bright region of “Area 2” in Figure 22.

Table 11. Summary tabular data for spectrum in Figure 23.

Element, Emission Line	Weight %	Atomic %	Net Intensity	Error %
C K	7.33	25.04	98.41	14.46
O K	0.87	2.23	47.22	22.52
Mg K	1.64	2.76	189.7	12.1
Al K	6.52	9.93	963.69	7.99
Si K	6.53	9.54	1165.74	7.13
Y L	8.11	3.75	692.68	6.41
P K	11.57	15.34	1896.39	6.12
Th M	3.11	0.55	227.4	10.53
La L	5.14	1.52	304.72	10.09
Ce L	9.45	2.77	536.56	6.85
Nd L	5.84	1.66	293.82	10.16
Fe K	33.89	24.91	2616.91	2.46

Figure 24 shows a BSE image of the smelted specimen at lower magnification, 200 μm length-scale, where several white areas of REE accumulation are visible.

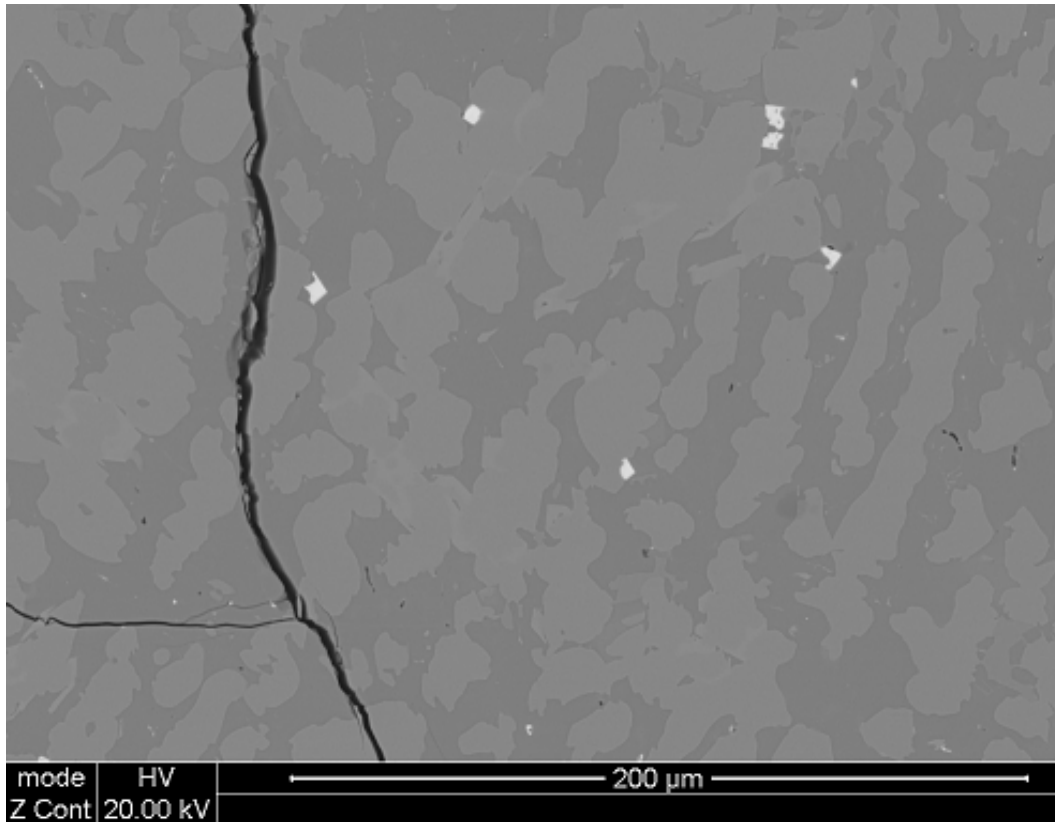


Figure 24. Lower magnification BSE image with several visible white areas of REE accumulation.

The darker, gray regions surrounding the bright areas were also analyzed for composition, and these were found to be various Si-Al-Fe phases containing no REE content. Figure 25 is an example spectrum for the darker regions around the bright region in the Area 2 view (Figure 25). The tabular results for the spectrum in Figure 25 are presented in Table 12.

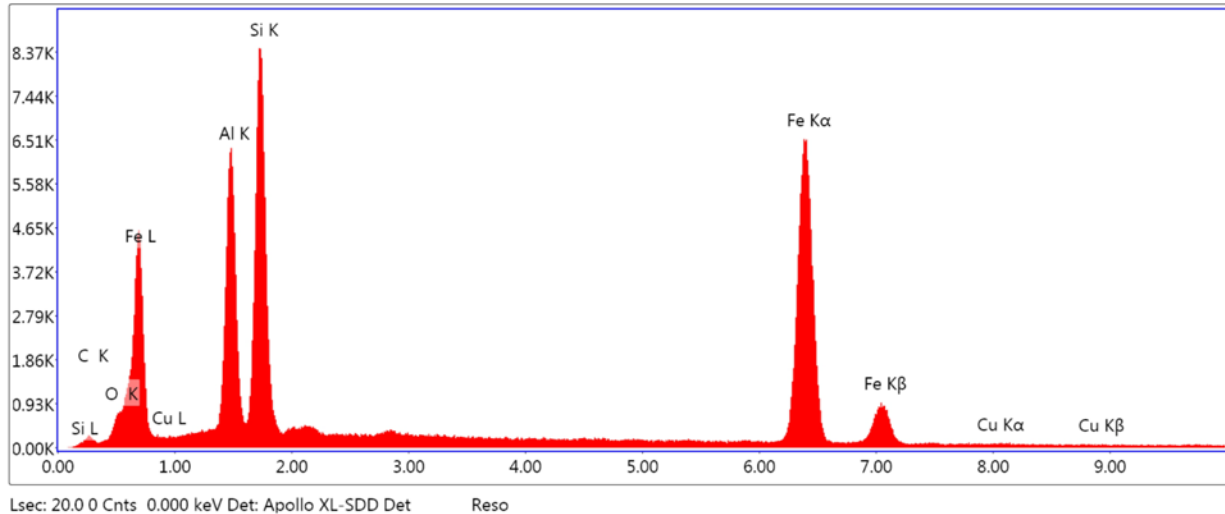


Figure 25. Spectrum for region outside of REE accumulation zone in Area 2, Figure 22.

Table 12. Summary tabular data for the spectrum in Figure 25.

Element, Emission Line	Weight %	Atomic %	Net Intensity	Error %
C K	7.47	20.17	104.85	13.36
O K	3.75	7.61	280.27	10.42
Al K	15.16	18.23	3011.06	6.71
Si K	19.59	22.63	4146.62	6.21
Fe K	53.6	31.14	4880.77	1.75
Cu K	0.43	0.22	22.78	46.24

For comparison, epoxy mounts of raw Williams Station ash (starting ash used for Tests 9 & 10) were also prepared for SEM-EDS analysis. Figure 26 presents BSE images of ash particles at the 100 μm length-scale and an individual ash particle at the 1 μm length-scale containing REE (bright “white” area circled in red). Tabular composition results from the EDS analysis of the circled area are given in Table 13. For the case of raw ash, the white areas were found to contain a high fraction of oxygen, $\sim 34\%$ by weight, and total REE content at $\sim 5\%$ for the Figure 26 example. This seems to confirm the expectation that REE occur as oxides in coal ash.

Generally, it was difficult to identify regions of REE content in the raw ash images. However, in comparing images showing regions of REE content – raw ash to smelted products – it is clear that the smelting process for Tests 9 and 10 was working to agglomerate REE into larger accumulation pockets as the REE content length-scales increased from $\sim 0.5 \mu\text{m}$ to as much as 20 μm (a ~ 40 -fold increase).

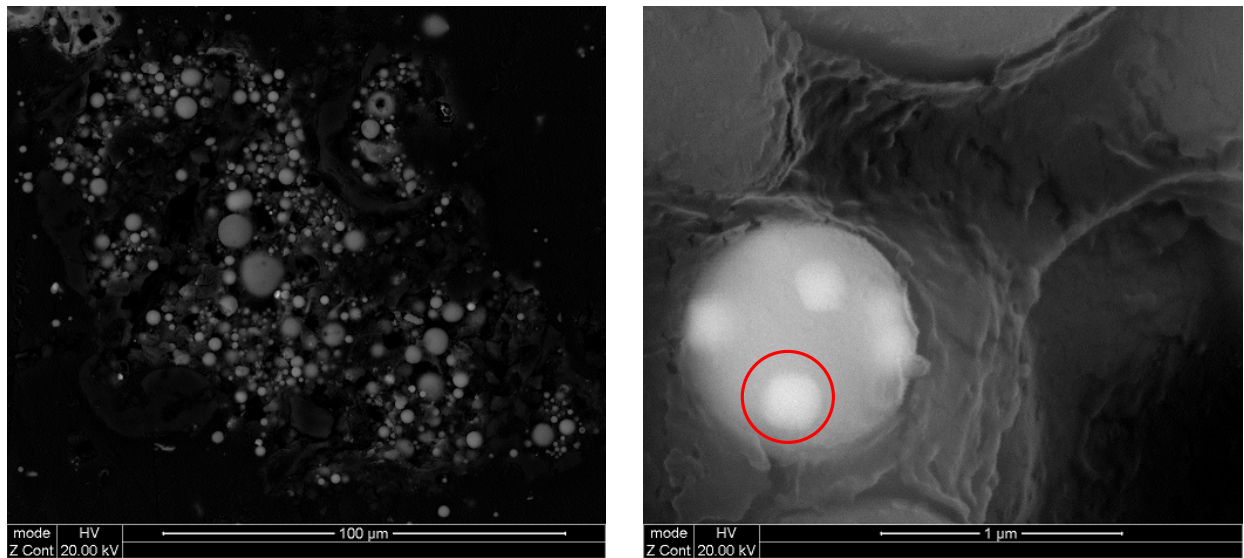


Figure 26. SEM BSE images of Williams Station fly ash (left) and a fly ash particle with REE accumulation – circled (right).

Table 13. Summary tabular data for the spectrum analysis of the circled region in Figure 26.

Element, Emission Line	Weight %	Atomic %	Net Intensity	Error %
C K	49.33	61.58	619.09	8.16
O K	33.75	31.63	508.41	10.03
Al K	4.52	2.51	425.31	5.42
Si K	4.97	2.66	513.79	4.43
P K	0.67	0.33	59.26	9.2
K K	0.29	0.11	23.18	14.41
Ca K	0.72	0.27	48.84	11.79
Ti K	0.44	0.14	24.99	15.77
La L	0.84	0.09	17.7	27.35
Ce L	3.2	0.34	64.54	12.38
Fe K	1.25	0.34	38.45	13.43

Summary observations from inspecting the SEM BSE images from the smelted specimens and the raw ash include the following:

- The bright white areas from the smelted specimens are likely solid crystals at the smelting temperature (2200 °C) growing from the melt as they have sharper well-defined boundaries.
- The length-scales of REE content areas increased significantly as a result of the modified smelting process, from sub 1 µm in raw ash to crystals in the range of 2–20 µm in the smelted specimens.
- A prominent phosphorus peak (P K – “K” emission) was always present with the REE crystals in the smelted specimens (see Figure 23).
- The darker Si-Al-Fe phases in the smelted specimens are likely molten at the smelting temperature as they have smooth, “roundish” boundaries.
- Generally, the smelted specimens contained only very low amounts of oxygen, which indicates the absence of a slag oxide phase – consistent with the observation of only a residual intermetallic product. It appears that all the oxygen was lost as CO from the carbothermic reduction reactions with the ash oxides. The loss of oxygen would also account for much of the sample mass loss during smelting.
- In contrast with REE content areas in raw ash, REE accumulation areas in the smelted specimens were also lacking in oxygen which seems to indicate the REE are present as a mixture of reduced metals as a result of the smelting process.

Finally, XRD analyses were performed on specimens from the Tests 9 and 10 products to determine the crystalline phases produced – especially to detect the presence of carbides – from the smelting process. Summary results are presented in Table 14.

Table 14. XRD results for Tests 9 and 10 specimens.

Phase	Test 9 Specimen, wt%	Test 10 Specimen, wt%
Amorphous	80.56	81.11
Quartz (SiO ₂)	1.00	0.89
Alabandite (MnS)	0.86	0.66
Almandine (Fe ₃ Al ₂ Si ₃ O ₁₂)	0.38	0.45
Iron-alpha (Fe)	9.14	8.85
Cohenite (Fe ₃ C)	7.08	6.66
Gehlenite (Ca ₂ Al)	0.17	0.18
Wadsleyite (Mg ₂ SiO ₄)	0.66	0.62

From Table 14, the smelting residuals are mostly amorphous (~80%), though this fraction appears to be a little higher as compared to raw ash. As could be expected, a significant iron rich phase is present (~9% Iron-alpha), and the smelting process appears to have produced some carbides with the presence of Cohenite (iron carbide – Fe₃C).

6. TEST UNIT DESIGN

As noted previously, completing the Task 4 activities to develop the vaporization/condensation option and prepare a detailed design package for a pilot-scale demonstration unit depended on a viable smelting process as originally proposed. The technology reassessment and resulting smelting process modifications could not be fully validated experimentally due to limitations of the testing equipment available to the project team. Therefore, faced with the combination of an unproven smelting process and inadequate equipment for validating modified concepts, the team abandoned designing a pilot-scale unit based on the original process options. Instead, a lab-scale test unit for further process development was designed which provides broad operating flexibility for conducting well-controlled experiments under a wide range of thermal and atmospheric conditions. This approach is prudent in that technology proof-of-concept can be more rigorously demonstrated for determining if pursuit of a pilot-scale system is warranted. The modified design concept is summarized further in the following sections.

6.1 Design Approach and Key Inputs

During the initial stages of testing for the Feasibility Study (Task 3), it became evident that both the Joule heating and plasma arc heating laboratory systems available for use were limited in their capabilities to provide necessary data and for demonstrating proof-of-concept. For example, the plasma system included a torch designed for a powder coating process. The high working gas velocity from the torch had a tendency to blow ash feedstock material out of the sample crucible during operation. Therefore, proximity of the sample to the plasma plume was critical – the sample needed to be close enough to be efficiently heated and melted, yet not too close for material to be ejected during testing. Other disadvantages associated with the plasma system included operating time limited to about one hour before equipment overheating and lack of provisions to measure temperatures inside the furnace or at the sample. Challenges associated with the available Joule heating systems included furnace dimensions that limited starting sample size and limitations on maximum operating time and temperature. Neither system enabled collection and sampling of vapors exiting the system, which was identified as a major source of potential data collection given the elevated temperature operation.

In an attempt to improve experimentation, a framework was developed for a testing system which incorporated the following considerations and key features:

- Provisions for increased control. For example, in previous experiments, violent reactions occurred at certain temperature intervals. Therefore, the proper heating rate and steady-state condition must be identified that minimizes losses, and this would require precise and repeatable control.
- Faster heating. This would allow for close simulation of rapid local heating encountered with a plasma arc system.
- Ability for testing with larger samples. The previous equipment limited sample sizes to ~35–40 g. Since ash REE concentrations are at the ppm level, sample amounts 10x that or more are preferable.
- Pneumatically ‘sealed’ environment and exhaust vapor scrubbing system to enable capture of more components leaving the crucible, thus ability to fully close the mass balance and improve both precision and accuracy as compared to what was done in previous experiments.
- Longer duration and higher temperature operation than previously possible with the current equipment.
- Joule heating operational mode to precisely control the heat input to the sample ash and control the phase-changing that occurs – critical for initial experiments.
- Electric arc heating option. The ability to test in this mode gives insight for the operation and performance of the intended technology for a commercial-scale installation.

Subsequently, a basic process flow diagram for a flexible test unit was prepared (presented in Figure 27).

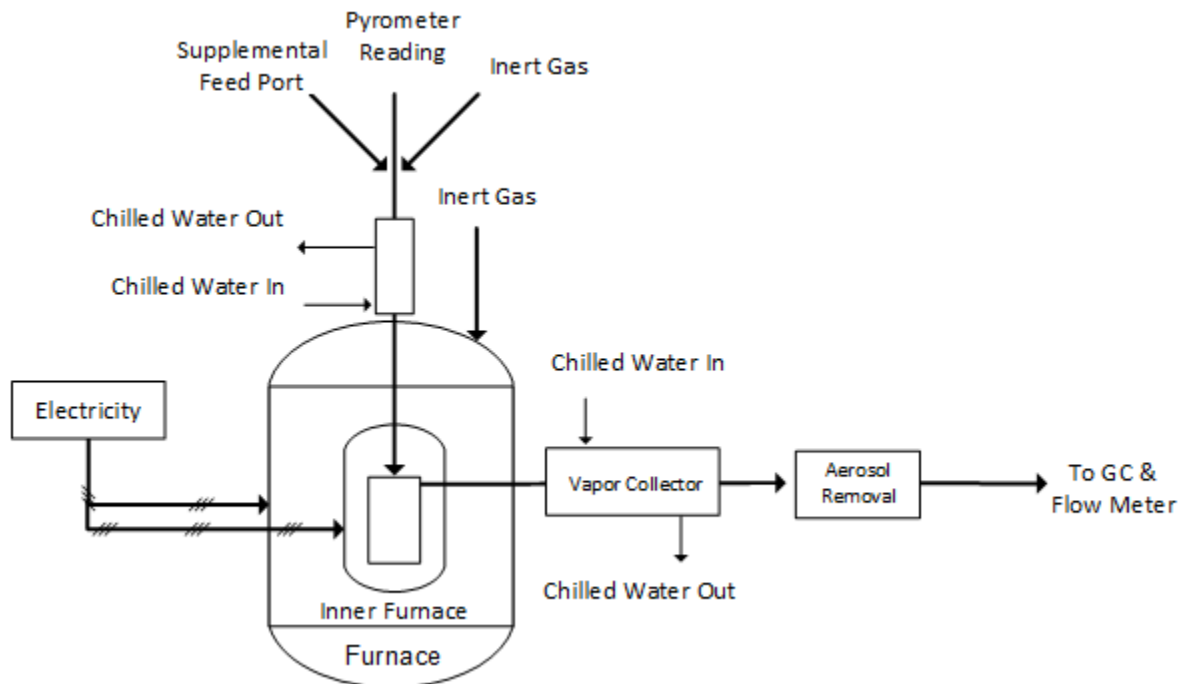


Figure 27. Process flow diagram for proposed flexible test unit.

An ash sample is prepared and sealed in the feed hopper located above the ash feed port. The crucible may be preloaded with ash as well, or it can be left empty and fed via the feed port once the system is at a desired temperature. The pyrometer orifice is also utilized as a feed tube and an inert gas inlet to the crucible. A water jacket maintains the feed port at lower temperatures until it enters the oven and inner furnace, where a graphite tube spans the remaining distance to the crucible, due to the potentially extreme temperatures ($>3000^{\circ}\text{C}$) experienced in the inner furnace. The ash sample is brought to a molten state – by either Joule heating or plasma arc heating – and decomposes inside the crucible. Gases produced during the smelting process – primarily carbon monoxide (CO) with small quantities of sulfur dioxide (SO₂) and any low boiling point metal vapors that break-through – are treated in an exhaust gas scrubbing system downstream from the furnace exit prior to final analysis by a GC and venting.

6.2 Design Concept and Specifications

The proposed flexible testing unit is composed of a conventional off-the-shelf high temperature laboratory furnace (hereby referred to as an oven for discussion simplicity), which has been modified to contain within its refractory walls a second heating section for ultra-high temperature operation. Two configurations are envisioned with this design: 1) a Joule heating system to enable finely controlled high temperature experiments, and 2) an electric arc system to complete the experiments required before constructing a pilot scale version of a plasma system. The Joule heating configuration is designed to enable finely controlled temperature experiments throughout a wide range of temperatures with reliable and accurate sample temperatures. This feature facilitates the critical step of confirming the conceptual approach based on the Ellingham diagram carbothermic reduction process.

The electric arc plasma process is intended to serve as a scaled-down version of the pilot methodology, in which an electric arc will be utilized for high efficiency thermal reduction of the feedstock based on the

carbothermic reduction proven with the first stage Joule heating process.

A steady state heat transfer analysis was performed to determine requirements on input power to the graphite heating element and insulation thickness. The temperature of the hot zone (inside the graphite heating element) was given at 2500°C, and the temperature of the cooler zone (commercial oven cavity) was assumed to be at 1600°C. The maximum heating power of the commercial oven is rated at 10 kW, which suggests this is the maximum power necessary to maintain 1600°C in the cooler zone and overcome all heat losses of the commercial oven itself. The inner graphite heating element was also designed to dissipate 10 kW so that when operating at steady state the standard oven elements can be nearly or completely powered down.

6.3 Preliminary Cost Estimates

A rough order of magnitude (ROM) budget was prepared for the proposed test system. The total ROM cost estimate to construct and set-up the system to rigorously evaluate pyrometallurgical treatments for concentrating REE from coal fly ash was ~\$150,000. The system budget was estimated based on discussion with vendors, quotes, and general experience with similar design and equipment specifications. Several suppliers of graphite components (pastes, insulation, cathodes, resistive elements, etc.) were identified and approached for quotes and pricing information for all the graphite components of interest in the inner furnace design. All modifications to the furnace (orientation, door mechanical design change, mass flow controller, feed system etc.) were calculated based on extensive internal experience with lab, bench, and pilot-scale design. Team member ArcSec Technologies was able to reference multiple past works in designing and constructing arc-style furnaces for validating many of the costs associated with the inner furnace design and construction. Typical costs for maintenance, programming and troubleshooting were also accounted for in addition to a basic 10% contingency cost.

7. CONCLUSIONS

Southern Research with project partners ArcSec and REI investigated pyrometallurgical treatments relying on plasma-arc technology for recovering and concentrating REE from post-combustion coal fly ash feedstocks. The proposed technology included a smelting process to separate ash into slag and reduced metal phases, where reduced REE were expected to partition to the metal phase. An additional follow-on process option specified vaporizing the reduced metal phase and condensing the vapors in sequential temperature ranges to separate individual REE components and produce additional REE-enriched metal fractions. The process is environmentally friendly in that the slag can be converted into benign salable products or disposed of as a highly stable waste residual, exhaust gases are scrubbed of hazardous pollutants, and large amounts of water and chemicals are not required.

Various coal ash samples were acquired and characterized for bulk oxide composition, REE content, metals content, and crystalline phases present. REE content ranged from 300–1200 ppm with average at 537 ppm. Ashes with the highest REE content were from Fire Clay coals of Central Appalachia (Eastern Kentucky). Generally, fly ash feedstocks were found to contain the “light” rare earths at 2–2.5 times that of the “heavy” rare earths.

During the feasibility study, it was demonstrated in bench-scale experiments that the smelting process could successfully separate ash into slag and reduced metal. However, REE collection in the metal phase was low – only concentrations of a few hundred ppm were achieved. Generally, the REE remained in the slag phase at concentrations similar to that of the raw ash feedstock. Equilibrium and computational modeling predicted that, assuming a viable smelting process, the vaporization/condensation process could achieve separation of individual REE and produce additional metal fractions, with higher REE enrichments. A simple economic analysis was used to determine the necessary value of products recovered from ash feedstocks for making a commercial installation profitable. However, there is much uncertainty on REE prices and the market value of low REE pre-concentrates.

During the second year of the project, the proposed recovery technology was reassessed, and the effort focused on determining how to improve the smelting process, since the subsequent project activities – developing the vaporization/condensation process and preparing a pilot-scale design package – depended on a viable smelting process operating as originally proposed. During a review of developed (or developing) applications of REE recovery from other waste streams that include pyrometallurgical processing, it was found that REE are usually preferentially collected in slag phases. Such practice is consistent with predictions on coal ash processing from the Ellingham diagram, which indicates that many of the REE components are much more stable as oxides as compared to the major ash constituent (Fe, Si, Al, and Ca) oxides. From the position of its curve on the diagram, iron oxide would readily be reduced to metal with increasing temperature. However, SiO_2 and some Al_2O_3 would preferentially be reduced to metals over most of the REE oxide species.

After comprehensive review of thermodynamic data, the first-year experimental results, and supplemental modeling results, the approach to the smelting process shifted to a strategy of sequentially reducing (carbothermally) the major ash oxide species (Fe, Si, etc.) and removing as much of them from the system as possible as metals, leaving behind the REE as oxides, more concentrated in the remaining slag phase.

To validate the adjusted smelting process approach, supplemental experiments were performed in the electric furnace using ash mixtures containing high carbon ratios to achieve highly reducing conditions.

Rather than separate slag and metal phases, however, the resulting product for these tests was a reduced Si-Al-Fe intermetallic residual. About 25–30% of the starting sample mass remained in the smelted product – much of the mass loss was likely oxygen, as CO produced from the carbothermic reactions with the ash oxides. REE recovery rates in the products ranged from 30–50% of that present in the starting sample mixtures. In some examples, the total REE content of the residual products was almost double that of the starting sample mixtures. When SEM-EDS analysis was performed on product specimens, pockets of REE agglomeration were identified. These appeared to be reduced metal crystals that grow during the ash melting process, having length-scales up to 20 μm and mixed REE content of 30 – 40% by weight. For comparison, areas of REE content were found in raw ash particles having length-scales of $\sim 0.5 \mu\text{m}$. Also in the raw ash, oxygen was associated with the REE content, which seemed to confirm the expectation that rare earths are present in ash as oxides. Therefore, in the limited experiments performed, the adjusted smelting process appears to have successfully reduced rare earth oxides to rare earth metals and concentrated the REE into phase-separated crystals. These “white” area crystals (as seen in the SEM images) have larger length-scales (up to 40x increase), and significantly more concentrated REE when compared to REE content in the original raw ash.

Faced with the combination of the unproven originally proposed smelting process and inadequate facilities for rigorously validating the modified approach, the project team abandoned preparation of a design for a pilot-scale demonstration unit. Instead, a lab-scale test unit for further process development was designed with features to allow broad operating flexibility for conducting well-controlled experiments under a wide range of thermal and atmospheric conditions. The design consists of a commercially available high temperature laboratory furnace modified to accommodate an inner heating section for ultra-high temperature operation. Provisions are included that allow for a Joule heating mode, to enable finely controlled temperature experiments, and a plasma arc heating mode, to simulate operation of the intended processing technology. Costs for the unit were estimated at $\sim \$150,000$. It is intended that this test unit would be a significant improvement over the currently available equipment for determining the necessary conditions to enhance REE extraction and recovery from coal ash using pyrometallurgical treatments.

Generally, the body of work completed for this project has greatly contributed to scientific research as there has been little similar experience and data available to draw upon for reference. Though the objective of extracting REE from coal fly ash into products with total mixed average REE concentrations approaching 2% has yet to be achieved using the proposed technology, smelted intermetallic residuals, containing phase-separated crystals with high weight fractions (up to 40%) of mixed REE metals, were produced. With further investigation, it is expected that the size of the REE-rich crystals can be enhanced, and the myriad of “white” crystals can be combined into much larger units producing metallic fractions with highly concentrated REE content, thus allowing the REE to be made more accessible to extraction in additional steps as part of a complex process. Other project accomplishments are also noteworthy. Analytical expertise and insight into reasonable expectations were gained through the creative use of the many techniques for characterizing feedstocks and products. Data was collected for varied approaches to pyrometallurgical separation treatments. Advancements in understanding the equilibrium behavior of vaporized species and developing techniques for modeling high temperature condensation processes were realized. Though limitations were encountered with available test equipment, the experience led to an improved system design, which includes features for experimental flexibility. With further development, it is expected that additional opportunities will be found to extend use of the technology to other commercial applications for the extraction and refinement of high-value and critical metals from nontraditional sources.

8. RECOMMENDED FUTURE WORK

With the most promising experimental performance achieved only recently by following the prescribed modified smelting approach – and near the end of the project period – the first priority for future work would be to construct the enhanced testing unit. With the more flexible and capable experimental facility, a broad test matrix could be developed and executed for determining the necessary processing conditions to prove whether or not the technology as envisioned is viable for extracting and concentrating REE from coal fly ash.

As was observed from the SEM-EDS analyses on product specimens from the later tests, the modified smelting process seemed to produce crystals containing a mixture of reduced rare earth metals with concentrations at 30–40% by weight and larger length-scales as compared to raw ash content. It should be determined if the processing conditions can be adjusted to achieve larger agglomerations and higher recovery yields. One consideration may include modifying the shape of the sample crucible. It is suggested that the use of a crucible designed with an acute-angled, cone-shaped bottom would promote gravity migration of the heavier REE crystals to collect into larger agglomerations at the crucible bottom. In previous DOE-supported work, transuranic waste was treated using plasma arc technology, and the collection of high purity metal alloys was enhanced using a long, narrow-bottomed crucible (Schumacher et al., 1995). It should also be determined if the form of smelted residual product and agglomerated crystals are more accessible to follow-on treatments to further isolate and collect the rare earth components. It may be that the larger length-scales/particle sizes produced make it easier to further liberate the REE content by other means. Ultimately, it may be possible to integrate the pyrometallurgical process with other physical separation or hydrometallurgical techniques for producing higher REE enrichments.

Another recommended key enhancement to the smelting process is to further develop the use of hydrogen plasma – only limited experiments were performed during the feasibility study with marginal success. Previously, it was noted that atomic hydrogen is a better reductant than carbon. The problem, though, is that molecular hydrogen gas (H_2) – a poor reductant – is the practical form of hydrogen that would be introduced into the system, and H_2 is thermodynamically stable up to 3500°C. However, H_2 can be fractionally converted to atomic, ionic, or other excited forms of hydrogen with introduction as a portion of the working gas in a plasma torch, where the plasma plume temperature would be well above 3500°C. Key advantages for replacing carbon with atomic hydrogen as the reductant include avoiding the production of carbides and a reduction in the smelting temperature (the hydrogen oxidation curve is lower on the Ellingham diagram relative to the carbon curve), which should also significantly reduce processing energy costs and minimize the amount of lower-boiling REE lost to vaporization.

Finally, the modified smelting approach also opens the door for new considerations. In the process of sequentially reducing metals, important economic incentives may legitimize a paradigm shift in the way resources such as coal are processed. For instance, Ca, Al, Si and other elements are highly valuable in their metal states, and are significant components of ash that could feasibly be separated as metal products. Also, processing the material at such high temperatures provides a high exergy value, which could be investigated using techno-economic analysis for recovering substantial amounts of sensible heat in addition to any thermochemical energy for maximizing processing efficiency. A broad ‘refinery’ concept that includes coal inputs in addition to low value ore or wastes may yield a high return on investment, but which will only be realized with further study and support from the scientific and industrial communities.

9. REFERENCES

- Blissett, R S, Smalley, N, & Rowson, N A. (2014). An Investigation into Six Coal Fly Ashes from the United Kingdom and Poland to Evaluate Rare Earth Element Content. *Fuel*, 119, 236-239.
- Borra, C R, Blanpain, B, Pontikes, Y, Binnemans, K, & Van Gerven, T. (2016a). Recovery of Rare Earths and Other Valuable Metals from Bauxite Residue (Red Mud): a Review. *Journal of Sustainable Metallurgy*, 2(4), 365-386.
- Borra, C R, Blanpain, B, Pontikes, Y, Binnemans, K, & Van Gerven, T. (2016b). Smelting of Bauxite Residue (Red Mud) in View of Iron and Selective Rare Earths Recovery. *Journal of Sustainable Metallurgy*, 2(1), 28-37.
- Firdaus, M, Rhamdhani, M A, Durandet, Y, Rankin, W J, & McGregor, K. (2016). Review of High-Temperature Recovery of Rare Earth (Nd/Dy) from Magnet Waste. *Journal of Sustainable Metallurgy*, 2(4), 276-295.
- Franus, W, Wiatros-Motyka, M M, & Wdowin, M. (2015). Coal Fly Ash as a Resource for Rare Earth Elements. *Environmental Science and Pollution Research*, 22(12), 9464-9474.
- Hallems, B, Wollants, P, & Roos, J R. (1995). Thermodynamic Assessment of the Fe-Nd-B Phase Diagram. *Journal of Phase Equilibria*, 16(2), 137-149.
- Hower, J C, Groppo, J G, Joshi, P, Dia, S, Moecher, D P, & Johnson, M N. (2013). Location of Cerium in Coal-Combustion Fly Ashes. *Coal Combustion and Gasification Products*, 5, 73-75.
- Ketris, M P, & Yudovich, Y E. (2009). Estimations of Clarkes for Carbonaceous Biolithes: World Averages for Trace Element Contents in Black Shales and Coals. *International Journal of Coal Geology*, 78(2), 135-148.
- Loginova, I V, Kyrchikov, A V, Lebedev, V A, & Ordon, S F. (2013). Investigation into the Question of Complex Processing of Bauxites of the Srednetimanskoe Deposit. *Russian Journal of Non-Ferrous Metals*, 54(2), 143-147.
- Mardon, S M, & Hower, J C. (2004). Impact of Coal Properties on Coal Combustion By-Product Quality: Examples From a Kentucky Power Plant. *International Journal of Coal Geology*, 59(3-4), 153-169.
- Mayfield, D B, & Lewis, A S. (2013). *Environmental Review of Coal Ash as a Resource for Rare Earths and Strategic Elements*. Paper presented at the 2013 World of Coal Ash Conference, Lexington, KY.
- Querol, X, Fernandez-Turiel, J, & Lopez-Soler, A. (1995). Trace Elements in Coal and their Behaviour During Combustion in a Large Power Station. *Fuel*, 74(3), 331-343.
- Report. (1997). Evaluation of Plasma Arc Technology for the Treatment of Municipal Solid Wastes in Georgia: The Construction Research Center, College of Architecture, Georgia Institute of Technology and the GTRI Environmental Science and Technology Program.
- Sabat, K C, Mishra, B K, & Rajput, P. (2014). Reduction of Oxide Materials by Hydrogen Plasma: An Overview. *Plasma Chemistry and Plasma Processing*, 34, 1-23.
- Schumacher, R F, Kielpinski, A L, Bickford, D F, Cicero, C A, Applewhite-Ramsey, A, Spatz, T L, & Marra, J C. (1995). *High-Temperature Vitrification of Low-Level Radioactive and Hazardous Wastes*. Paper presented at the International Symposium on Environmental Technologies: Plasma Systems and Applications, Atlanta, GA.
- Seredin, V V, & Dai, S. (2012). Coal Deposits as Potential Alternative Sources for Lanthanides and Yttrium. *International Journal of Coal Geology*, 94, 67-93.
- Tang, K, Ciftja, A, Martinez, A M, van der Eijk, C, Bian, Y, Guo, S, & Ding, W. (2014). Recycling the Rare Earth Elements from Waste NiMH Batteries and Magnet Scraps by Pyrometallurgical Processes.
- Verhaeghe, F, Goubin, F, Yazicioglu, B, Schurmans, M, Thijs, B, Haesebroek, G, . . . Van Camp, M. (2011). *Valorisation of Battery Recycling Slags*. Paper presented at the 2nd International Slag Valorization Symposium, Leuven, Belgium.